15320

rvices Technical Information Agency

Reproduced by

DOCUMENT SERVICE CENTER

KNOTT BUILDING, DAYTON, 2, OHIO

UNCLASSIFIED

DISCLAIMER NOTICE

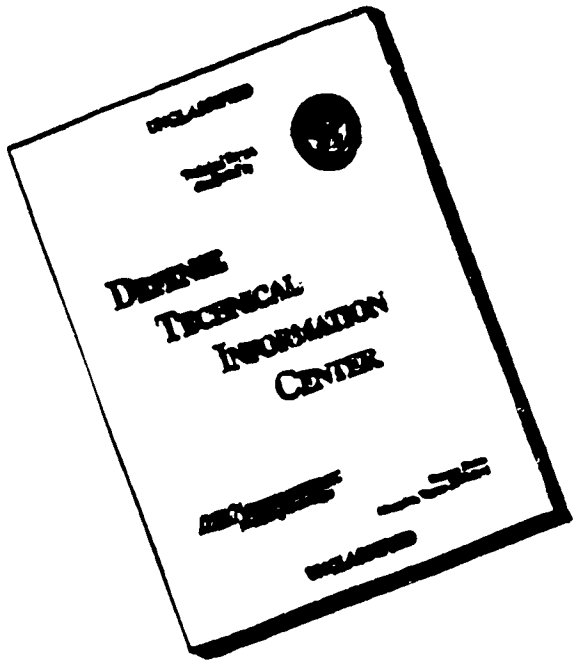

THIS DOCUMENT IS BEST QUALITY AVAILABLE. THE COPY FURNISHED TO DTIC CONTAINED A SIGNIFICANT NUMBER OF PAGES WHICH DO NOT REPRODUCE LEGIBLY.

NAVORD REPORT 3854

FC

A THEORETICAL INVESTIGATION OF TURBULENT BOUNDARY LAYER FLOW WITH HEAT TRANSFER AT SUPERSONIC AND HYPERSONIC SPEEDS

19 MAY 1955

U. S. NAVAL ORDNANCE LABORATORY
WHITE OAK, MARYLAND

NAVORD Report 3854

Aeroballistic Research Report 258

A THEORETICAL INVESTIGATION OF TURBULENT BOUNDARY LAYER FLOW WITH HEAT TRANSFER AT SUPERSONIC AND HYPERSONIC SPEEDS

Prepared by:

Jerome Persh

ABSTRACT: A theoretical investigation of compressible turbulent boundary layer flow with and without steady state heat transfer has been conducted. This investigation is based on a simple physical model of the flow suggested first by Prandtl and used later by Donaldson. The physical model consists of a laminar sublayer region with a linear velocity profile and an outer turbulent portion with a power law velocity profile. Comparisons between theory and experiment demonstrate that the analysis yields good results for compressible turbulent boundary layer flow with and without steady state heat transfer.

U. S. NAVAL ORDNANCE LABORATORY
WHITE OAK, MARYLAND

NAVORD Report 3854 19 May 1955

This report contains the results of a theoretical investigation of compressible turbulent boundary layer flow with and without steady state heat transfer. The significance of this work is apparent when it is considered that although a great deal of experimental and theoretical information exists for supersonic turbulent boundary layers in the absence of heat transfer, there are relatively few detailed investigations in the supersonic and hypersonic speed ranges that include the effects of heat transfer.

The work was jointly sponsored by the U. S. Naval Bureau of Ordnance and the U. S. Air Force, and was performed under Tasks NOL-M9a-133-1-55 and NOL-M9a-133-5-55. The author is deeply indebted to Dr. R. E. Wilson and Dr. R. K. Lobb for their guidance and continued interest during the course of the investigation, and to Mrs. Leah Brown of the Applied Mathematics Division, who carried out the computation of the data contained in Table I.

JOHN T. HAYWARD
Captain, USN
Commander

H. H. KURZWEG, Chief
Aeroballistic Research Department
By direction

CONTENTS

ILLUSTRATIONS

SYMBOLS

c_f = Local skin friction coefficient based on free-stream conditions, $2\tau_w/\rho_\infty u_\infty^2$

C_F = Mean skin friction coefficient based on free-stream conditions, $\frac{2D}{\rho_\infty u_\infty^2 x}$

c_{fi} = Incompressible local skin friction coefficient for zero heat transfer based on free-stream conditions

C_{Fi} = Incompressible mean skin friction coefficient for zero heat transfer based on free-stream conditions

D = Drag force

H = Boundary layer shape parameter, δ^*/θ

k = Constant in mixing length law

ℓ = Mixing length

M = Mach number

n = Exponent in power law velocity profile representation

r = Ratio of total shear stress to viscous shear stress

r.f. = Recovery factor

Re = Reynolds number

T = Local static temperature

u = Mean velocity component in x-direction

u^+ = Velocity parameter, u/u_τ (based on wall conditions)

u_τ = Friction velocity $\sqrt{\tau_w/\rho_w}$

x = Axial distance along surface

y = Distance perpendicular to surface

y^+ = Wall distance parameter, yu_τ/ν (based on wall conditions)

SYMBOLS (continued)

δ = Total boundary layer thickness

δ^* = Boundary layer displacement thickness, $\int_0^{\delta} \left[1 - \frac{\rho u}{\rho_\infty u_\infty} \right] dy$

θ = Boundary layer momentum thickness, $\int_0^{\delta} \frac{\rho u}{\rho_\infty u_\infty} \left[1 - \frac{u}{u_\infty} \right] dy$

μ = Viscosity

ν = Kinematic viscosity

ρ = Density

$\tau_{Lam.}$ = Laminar shear stress

$\tau_{Turb.}$ = Turbulent shear stress

ω = Exponent in viscosity-temperature relationship

Subscripts:

e = Equilibrium wall temperature

L = Values at the edge of laminar sublayer

T = Turbulent region

w = Values based on wall conditions

x = Values based on distance from leading edge of plate

δ = Values based on boundary layer thickness

θ = Values based on boundary layer momentum thickness

∞ = Values based on free-stream conditions outside boundary layer

NAVORD Report 3854

A THEORETICAL INVESTIGATION OF TURBULENT BOUNDARY LAYER FLOW WITH HEAT TRANSFER AT SUPERSONIC AND HYPERSONIC SPEEDS

INTRODUCTION

1. Despite a lack of experimental data, numerous formulae have been developed for the variation of turbulent skin friction on a flat plate, with and without steady state heat transfer. The reports of Rubesin, Maydew, and Varga (reference a), and Chapman and Kester (reference b) include good resumes of several theoretical treatments of this problem. All of the analyses reviewed in these references make use of empirical constants which are drawn from incompressible experimental data. Recent experimental results (reference c) have demonstrated that the empirical incompressible constants utilized are affected by heat transfer. Specifically, it has been found that the assumption that the edge of the laminar sublayer occurs at fixed values of the parameters u_L^+ (or y_L^+) is not strictly valid. Experimental results indicate that the value of u_L^+ does not only vary with heat transfer, but to some extent with Reynolds number and Mach number. It was felt, therefore, that a theoretical approach which is based on a realistic physical model of the flow, and which allows a prediction of the quantities at the edge of the laminar sublayer, is expedient at the present time.

2. Such an approach was originally devised by Prandtl (reference d) and recently extended to compressible flows by Donaldson (reference e) The physical model of a turbulent boundary layer proposed by these investigators may be briefly described as follows: It is assumed that the turbulent boundary layer velocity profile can be divided into two regions; the wall adjacent region called the laminar sublayer, where the velocity varies linearly with distance from the surface, and the outer turbulent portion, which is represented by a power profile. The intersection of these two profiles is defined as the edge of the laminar sublayer.

3. It is the purpose of this investigation to extend and revise the analysis of Donaldson in order to obtain consistency with the most recent and reliable experimental results for low speed turbulent boundary layers. The applicability of this analysis for compressible turbulent boundary layers with and without steady state heat transfer is demonstrated by comparisons with supersonic and hypersonic experimental results.

ANALYSIS

Incompressible Turbulent Boundary Layers

4. It has been established by numerous investigators that the velocity profile in the outer turbulent portion of the boundary layer may be adequately represented by a power profile of the form

$$\frac{u}{u_\infty} = \left[\frac{y}{\delta}\right]^{\frac{1}{n}} \qquad \delta_L \leq y \leq \delta \tag{1}$$

while experimental evidence indicates that, in the laminar sublayer region, the velocity profile is essentially a straight line

$$\frac{u}{u_L} = \frac{y}{\delta_L} \times \text{constant} \qquad o \leq y \leq \delta_L \tag{2}$$

The boundary layer is thus divided into a turbulent portion described by Eq. (1) and a laminar region having a linear velocity profile (Eq. 2). This is shown in Figure 1 with the real conditions in the transition region indicated by a dashed line.

5. Several general relations for the local skin friction coefficient can be deduced using the preceding postulates regarding the boundary layer velocity profile together with various assumptions regarding the shear stress at the edge of the laminar sublayer. These relations necessarily embody unknown functions which must be evaluated empirically.

6. Donaldson (reference e) introduced an empirical constant relating the total shear stress and the laminar shear stress in order to compute the skin friction. Taking

$$\frac{\tau_{\text{Lam.}} + \tau_{\text{Turb.}}}{\tau_{\text{Lam.}}} = r = \text{constant} \tag{3}$$

and evaluating r at $y = \delta_L$ from the power profile given by Eq. (1), Donaldson (reference e) derived the following relation for the skin friction coefficient

$$c_{f1} = 2\left[\frac{n(r-1)}{k^2}\right]^{\frac{1-n}{1+n}}\left[\frac{1}{Re_\delta}\right]^{\frac{2}{n+1}} \tag{4}$$

and evaluated the constant $(r-1)/k^2$ empirically using Blasius' (reference d) skin friction law. In Donaldson's analysis, the velocity profile exponent (n) is considered constant, and the Prandtl mixing length law

$$\ell = k\,y \tag{5}$$

is assumed in order to calculate the turbulent shear stress, $\tau_{Turb.}$*

7. In the present report the velocity profile exponent (n) was taken as a variable and the method by which Eq. (4) was correlated with experiment is as follows: First, Eq. (4) was equated to the Karman-Schoenherr incompressible skin friction law

$$c_{fi} = \frac{0.0568}{\left[\mathrm{Log}_{10}\,(2\mathrm{Re}_\theta)\right]\left[\mathrm{Log}_{10}\,(2\mathrm{Re}_\theta) + 0.868\right]} \tag{6}$$

which is regarded as a good representation of incompressible turbulent boundary layer skin friction coefficients over a wide Reynolds number range. This procedure yielded a variation of n with Re_θ. A comparison was then made between experimental data and the deduced variation of n with Re_θ. This approach seemed logical because the experimental variation of n with Re_θ is well

---

* An examination of Figure 2 suggests that since the shear stress is nearly constant near the wall, an alternate assumption regarding the relationship between the laminar and turbulent shear stress may be made. Within the sublayer the laminar shear stress predominates while outside the sublayer the turbulent shear stress predominates, and since the transition region is neglected in the model for the velocity profile, the values of $\tau_{Turb.}$ calculated from Eq. (1) and $\tau_{Lam.}$ calculated from Eq. (2) may be taken as each equal to the total shear stress at $y = \delta_L$. Thus a logical relationship between $\tau_{Turb.}$ and $\tau_{Lam.}$ would appear to be

$$\tau_{Turb.} = \tau_{Lam.} \text{ at } y = \delta_L$$

if $\tau_{Turb.}$ and $\tau_{Lam.}$ are computed as indicated above. In addition, if the von Karman mixing length formula

$$\ell = k\,\frac{\frac{du}{dy}}{\frac{d^2u}{dy^2}}$$

is used instead of the Prandtl mixing length formula, each of the shear stress assumptions will lead to another skin friction relation.

A study was therefore made to determine which of the assumptions and mixing length formula yielded a skin friction law which gave the best overall agreement between theory and experiment. It was found that Eq. (4) given by Donaldson, could best be adapted to the experimental results. The details of this analysis are contained in Appendix A.

described by a large amount of experimental velocity profile data. It was found that using this procedure and taking $\frac{r - 1}{k^2}$ as constant resulted in a variation of n with Re_θ which is a good average of the available experimental data (references c, f, g, and h). This is shown in Figure 3. The value of the constant $\frac{r - 1}{k^2}$ compatible with the n variation with Re_θ shown in Figure 3 is 20.0. This is only slightly different from the value of 22.5 given by Donaldson (reference e). Since in his analysis the n variation with Reynolds number was not considered and the Blasius (reference d) skin friction law was used to obtain the constant, it is to be expected that a slightly different constant would be obtained. The incompressible portion of the present analysis therefore represents an extension of the Donaldson analysis in that the n variation with Reynolds number is considered.

Compressible Turbulent Boundary Layers

8. Since for compressible flow, the temperature varies across the boundary layer, it is apparent that the assumption of constant shear stress through the laminar sublayer violates the stipulation that the velocity varies linearly with distance from the surface. It is assumed that this incompatibility does not introduce any serious errors in the skin friction results. The subsequent comparisons between theory and experiment tend to confirm this assumption.

9. The extension of the foregoing analysis to compressible flows is straightforward and the equations take the same form as those given in reference (e). If the value of the constant r obtained by the procedure described above is assumed to be the same for both incompressible and compressible flows with and without heat transfer, then Eq. (4) is valid for these cases if the density and viscosity contained in the Reynolds number are evaluated at the edge of the laminar sublayer. It is desirable, however, that the Reynolds number be expressed in terms of free-stream properties. This transformation is presented in reference (e) and in Appendix B where it is shown that the resulting equations necessary to determine local skin friction coefficients are as follows:

$$c_f = 2\left[20\ n\right]^{\frac{1-n}{1+n}}\left[\frac{1}{Re_\theta\left(\frac{\delta}{\theta}\right)}\right]^{\frac{2}{n+1}}\left[\frac{T_\infty}{T_L}\right]^{\frac{n-2\omega-1}{n+1}} \tag{7}$$

$$\frac{T_L}{T_\infty} = 1 + r.f.\frac{\gamma-1}{2}M_\infty^2\left[1-\left(\frac{u_L}{u_\infty}\right)^2\right] + \frac{T_w - T_e}{T_\infty}\left[1 - \frac{u_L}{u_\infty}\right] \tag{8}$$

$$\frac{u_L}{u_\infty} = \left[\frac{20\,n}{Re_\theta \left(\frac{\delta}{\theta}\right)}\right]^{\frac{1}{n+1}} \times \left\{1 + r.f.\,\frac{\gamma - 1}{2} M_\infty^2 \left[1 - \left(\frac{u_L}{u_\infty}\right)^2\right] + \frac{T_w - T_e}{T_\infty}\left[1 - \frac{u_L}{u_\infty}\right]\right\}^{\frac{1.76}{n+1}} \qquad (9)$$

10. Values of n for use in these equations are obtained from the curve of Figure 3. Using this single curve as a determining factor for n implies that n is uniquely related to Re_θ regardless of Mach number or heat transfer condition. Although the results shown in Figure 3 tend to justify this postulate, probably the Mach number and heat transfer influences on n are concealed by the insensitivity inherent in this coordinate system. A comparison between a plot of n versus Re_θ and n versus Re_δ indicates that some influence of Mach number and heat transfer is probably incorporated in both figures, but is appreciably less in the Re_θ plot. It is felt, therefore, that a more accurate determination of n may be obtained when Re_θ is used as the correlating factor.

11. Since Re_θ was chosen as the correlating factor for n and Eq. (7) requires the use of Re_δ, a means is therefore needed for converting given values of Re_θ to the equivalent Re_δ. The needed θ/δ values have been calculated using the definition for θ with Eq. (1) and the Crocco temperature distribution (reference e) for a series of Mach numbers up to 20, a wide range of heat transfer conditions, and n values of 5, 7, 9, and 11. These are tabulated in Table I. Also tabulated for the same range of variables are the values of δ^*/δ and H. It should be noted that the foregoing procedure for calculating these parameters ignores the laminar sublayer because the power profile is assumed to exist to the wall. While this procedure is not quite exact, it is felt that only small errors will result because by far the largest contributions to the integrals for δ^* and θ occur outside the laminar sublayer.

12. Using the present analysis, skin friction coefficients can be calculated if the Reynolds number is given in terms of either the total boundary layer thickness (Re_δ) or the boundary layer momentum thickness (Re_θ), or, as will be shown later, in terms of the distance from the leading edge. Since the dependence of θ/δ with Mach number and heat transfer is not considered in Donaldson's (reference e) analysis, the skin friction coefficient can be evaluated only if the value of Re_δ is known.

13. Whether or not the postulated uniqueness of n with Re_θ leads to serious errors may be checked by comparing the influence of n on c_f over a range of Mach numbers for a fixed value of Re_θ. A value of Re_θ of 8000 was selected for the check procedure,

and the n value was varied between 5.5 and 7.5 which encompasses the scatter of the experimental data at this point. It was found that the values of c_f over a range of Mach numbers up to 10 were no more than 6 percent above or below the curve drawn for the value of n theoretically associated with an Re_θ of 8000. On the basis of this check it was concluded that the skin friction values obtained from the present analysis are not particularly sensitive to the value of n associated with the Re_θ in question.

14. This result enables the approximate calculation of the variation of c_f/c_{fi} as a function of Re_x. If c_f/c_{fi} is not particularly sensitive to n, it may be assumed that for a given Mach number and heat transfer rate, the value of θ/δ along a plate is constant. This assumption is necessary to perform the integration indicated in Appendix C. Using this assumption, a relation between Re_δ and Re_x may be deduced. The details of this derivation are given in Appendix C, where it is shown that the resulting equation is

$$Re_\delta = Re_x^{\frac{n+1}{n+3}} \times \left\{ \left(\frac{\delta}{\theta}\right)^{n+1} \left(\frac{n+3}{n+1}\right)^{n+1} \left(\frac{1}{20n}\right)^{n-1} \left(\frac{T_\infty}{T_L}\right)^{n-2.52} \right\}^{\frac{1}{n+3}} \qquad (10)$$

It is not stipulated, however, that the value of (n) for use in equation (10) is a constant. Curves showing the variation of c_f/c_{fi} as a function of Mach number for several constant values of wall temperature ratio and a constant value of Re_x of 10^7 (Figure 15) calculated using the equations of Appendix C are in good agreement with the empirical curves of Seiff (reference a). Results obtained using the equations of Appendix C should therefore suffice for most engineering applications.

15. The recent acquisition of detailed experimental data at hypersonic Mach numbers at both the Naval Ordnance Laboratory and the Applied Physics Laboratory (references c and f), both with and without steady state heat transfer, made it possible to examine not only the overall results of the theory but also the validity of the assumptions made and the use of constants drawn from incompressible flow results.

16. The first step is to examine the conditions at the edge of the laminar sublayer. This is necessary because the theory is focused on this point. For incompressible flows it has long been assumed that the value of $u_L^+ = y_L^+$ at the edge of the laminar sublayer (in the logarithmic velocity profile representation) is roughly a constant that lies between 11.0 and 12.0. The present analysis is not based on this assumption but is so constructed that a computation and check of the results obtained for this point may be made.

17. The theoretical variation of u_L^+ with Re_θ is compared with experimental data (references i and j) for incompressible flow in Figure 4. It is apparent that the accepted presumption that $u_L^+ - y_L^+$ is a constant is not far from true; however, the theory and experiment indicate that Reynolds number does influence the value of $u_L^+ - y_L^+$ slightly.

18. Figure 5 shows a comparison between the theoretical and experimental values (references c, f, and k) of $u_L^+ - y_L^+$ for compressible flow. For this comparison all values of $u_L^+ - y_L^+$ are based on wall properties. The theoretical curves associated with each set of experimental data were calculated such that they encompassed the experimental Mach number and Reynolds number range. Although the present analysis does not accurately predict the numerical values of $u_L^+ - y_L^+$ it does predict the proper trend of the data for both the heating and cooling cases.

19. In the formulation of this analysis, the incompressible skin friction law of Karman-Schoenherr has been used as a basis for the zero heat transfer case. Unfortunately, little experimental data are available which describe the influence of heat transfer on incompressible skin friction coefficients. The analysis can, however, be applied to this case and comparisons made with the few data that are available. The experimental results of reference (l), while not reported in sufficient detail to make an exact computation using the present analysis, may be used to show that it does predict qualitatively correct results. In using these experimental data for this comparison it is assumed that the ratio c_f/c_{fi} can be used interchangeably with C_F/C_{Fi} and that little Reynolds number dependence on this ratio exists. Figure 6 shows both the predicted and experimental variation of c_f/c_{fi} with wall temperature ratio for a constant value of Re_θ which represented a mean for the data of reference (l). The results shown in this figure demonstrate that the present analysis describes correctly the variation of c_f/c_{fi} with increasing wall temperature ratio. Figure 7 shows the influence of heat transfer parameter on the values of c_f/c_{fi} for several values of Mach number and a single value of Re_θ. It is apparent that cooling of the surface results in an increase in the skin friction coefficient, whereas heating has the opposite effect. That this result is consistent with the incompressible results shown in Figure 6 is evident from the results shown in Figure 8. This figure shows the variation of c_f/c_{fi} with Mach number for several constant values of T_w/T_∞. The curves of constant T_w/T_∞ intercept the zero heat transfer curve at only one point. Each intercept occurs at the Mach number where $T_w/T_\infty = T_e/T_\infty$. A curve of the same appearance has been deduced by Seiff (reference m) from an empirical correlation of experimental data for Mach numbers up to about 5. A direct comparison between the results presented in Figure 8 and those reported in reference(m) is not valid because the curves of Figure 8 were computed for constant Re_θ and depend somewhat on this Reynolds number, whereas those of reference(m) are assumed to be independent of Reynolds number based on distance from the leading edge.

20. A comparison between specific values of experimental skin friction coefficients and the associated values predicted by the present analysis is shown in the following three figures. Figure 9 shows the variation of c_f/c_{fi} with Mach number for zero heat transfer. All of the experimental data (references a, b, c, f, k, n, o, and p) shown were normalized to a constant Re_θ of 8000 and are either specifically for the case of zero heat transfer or were linearly extrapolated to the zero heat transfer condition. The scheme used for processing the heat transfer results is outlined in reference (c). Good agreement between theory and experiment is found for the entire range of Mach numbers for which experimental data are available. Figures 10 and 11 show comparisons between theoretical and experimental values of c_f/c_{fi} plotted as a function of heat transfer parameter for those experimental data taken under conditions of steady state heat transfer (references c, f, and k). For each of the sets of data shown, the variation of Reynolds number with heat transfer rate, if any, was considered in the theoretical calculations. It is significant to note that the results shown for the data of reference (c) indicate little variation of skin friction ratio with increasing heat transfer. From the present analysis it appears that the increase in Reynolds number, which accompanied the increase in heat transfer rate, so influenced the results as to obviate any increase in skin friction ratio. In general, the agreement between theory and experiment is satisfactory for each of the sets of data shown.

CONCLUDING REMARKS

21. A theoretical investigation of compressible turbulent boundary layers with heat transfer has been conducted. This investigation is based on a simple flow model which is realistic for both the zero heat transfer and heat transfer conditions. The validity of the flow model assumed is demonstrated by comparisons between theoretical and experimental results. The theory is presented in such a fashion that values of skin friction may be calculated when either the Reynolds number based on boundary layer momentum thickness, total boundary layer thickness, or distance from the leading edge is given. Good agreement is demonstrated between theoretical and experimental values of skin friction coefficients, for both the zero and heat transfer conditions. It is shown that the predicted influence of heat transfer and Reynolds number on the properties at the edge of the laminar sublayer is consistent with the available experimental data for both incompressible and compressible flows. It is anticipated that, with the acquisition of additional data covering a broader range of conditions, improvements will be made in both the functional nature and accuracy of the analysis.

REFERENCES

(a) Rubesin, M. W., Maydew, R. C., and Varga, S. A., "An Analytical and Experimental Investigation of the Skin Friction of the Boundary Layer on a Flat Plate at Supersonic Speeds," NACA TN 2305, February 1951.

(b) Chapman, Dean R. and Kester, Robert H., "Measurements of Turbulent Skin Friction on Cylinders in Axial Flow at Subsonic and Supersonic Velocities." Paper presented at 21st Annual Meeting, I.A.S., New York, N.Y. January 26-29, 1953 (Preprint No. 391).

(c) Lobb, R. K., Winkler, E. M., and Persh, Jerome, "Experimental Investigation of Turbulent Boundary Layers in Hypersonic Flow," NAVORD Report 3880, February 1955.

(d) Prandtl, L., "The Mechanics of Viscous Fluids," Vol. III, Aerodynamic Theory, W. F. Durand, editor, 1943.

(e) Donaldson, C. Du P., "Skin Friction and Heat Transfer through Turbulent Boundary Layers for Incompressible Flows and Compressible Flows" (presented at the Heat Transfer and Fluid Mechanics Institute Meeting in Los Angeles, Calif., June 1952).

(f) Hill, F. K., "Boundary-Layer Measurements in Hypersonic Flow" (to be published in the Journal of Aeronautical Sciences).

(g) Ross, Donald, "A Study of Incompressible Turbulent Boundary Layers," Technical Memorandum, ONR Project NR 062-139-1, Ordnance Research Laboratory, The Pennsylvania State College, School of Engineering, State College, Pennsylvania, June 1953.

(h) Wilson, R. E., "Turbulent Boundary Layer Characteristics at Supersonic Speeds --Theory and Experiment," J. Aeronaut. Sci., Vol. 17, No. 9, p. 585, September 1950.

(i) Ross, Donald, "Turbulent Flow in Smooth Pipes --A Reanalysis of Nikuradses' Experiments," Ordnance Research Laboratory, The Pennsylvania State College, State College, Pennsylvania, Serial No. NOrd 7958-246, September 1952.

(j) Laufer, John, "Investigation of Turbulent Flow in a Two-Dimensional Channel," NACA Report 1053, 1951.

(k) Monaghan, R. J. and Cooke, J. R., "The Measurement of Heat Transfer and Skin Friction at Supersonic Speeds. Part III - Measurements of Overall Heat Transfer and of the Associated Boundary Layers on a Flat Plate at M = 2.43," R. A. E. Tech. Note No. AERO 2127, Dec. 1951.

(l) Humble, Leroy V., Lowdermilk, Warren H., and Desmon, Leland G., "Measurements of Average Heat Transfer and Friction Coefficients for Subsonic Flow of Air in Smooth Tubes at High Surface and Fluid Temperatures," NACA Report 1020, 1951.

(m) Seiff, Alvin, "Examination of the Existing Data on the Heat Transfer of Turbulent Boundary Layers at Supersonic Speeds form the Viewpoint of Reynolds Analogy," NACA TN 3284, August 1954.

(n) Coles, Donald, "Measurements in the Boundary Layer on a Smooth Flat Plate in Supersonic Flow," Thesis, California Institute of Technology, May 1953.

(o) Brinich, Paul F. and Diaconis, Nick S., "Boundary Layer Development and Skin Friction at a Mach Number 3.05," NACA TN 2742, 1952.

(p) Korgeki, R. H., "Transition Studies and Skin Friction Measurements on an Insulated Flat Plate at a Hypersonic Mach Number," California Institute of Technology, Guggenheim Aeronautical Laboratory, Hypersonic Wind Tunnel, Pasadena, California, Memorandum No. 17, July 1954.

(q) Weiler, T. E. and Hartwig, W. H., "The Direct Measurement of Local Skin Friction Coefficient," Report CF-174,, DRL-295, Defense Research Laboratory, University of Texas, Austin, Texas, September 1952.

APPENDIX A

General Relations for the Local Skin Friction Coefficient

1. The equation of motion to be satisfied by a boundary layer flowing on a flat plate in the absence of a pressure gradient is:

$$u\frac{du}{dx} + v\frac{du}{dy} = \frac{1}{\rho}\frac{d\tau}{dy} = \frac{1}{\rho}\frac{d}{dy}\left[\mu\frac{du}{dy} + \rho\ell^2\left(\frac{du}{dy}\right)^2\right] \tag{A1}$$

The total shear stress at any point in the boundary layer is

$$\tau_{Lam.} + \tau_{Turb.} = \mu\frac{du}{dy} + \rho\ell^2\left(\frac{du}{dy}\right)^2 \tag{A2}$$

Donaldson (reference e) assumed that the ratio of the total stress to the laminar stress at the edge of the laminar sublayer is a constant,

$$\frac{\tau_{Lam.} + \tau_{Turb.}}{\tau_{Lam.}} = r = \text{constant} \quad \text{at } y = \delta_L \tag{A3}$$

Using this assumption, and evaluating Eq. A2 at $y = \delta_L$ by using,

$$\frac{du}{dy} = \frac{u_\infty \delta_L^{\frac{1-n}{n}}}{n\,\delta^{1/n}} \tag{A4}$$

which is obtained from the power profile (Eq. 1), it can be shown that the thickness ratio of the laminar sublayer is

$$\frac{\delta_L}{\delta} = \left[\frac{n(r-1)\,\delta_L^2}{\ell^2\ Re_\delta}\right]^{\frac{n}{n+1}} \tag{A5}$$

2. It may also be logically assumed that at $y = \delta_L$, the laminar shear stress is equal to the turbulent shear stress

$$\tau_{Lam.} = \tau_{Turb.} \quad \text{at } y = \delta_L$$

Evaluating $\tau_{Turb.}$ using Eq. 1 and $\tau_{Lam.}$ using Eq. 2 yields the following expression for the thickness ratio of the laminar

sublayer

$$\frac{\delta_L}{\delta} = \left[\frac{n^2\,\delta^2}{\ell^2}\,\frac{1}{Re_\delta}\right]^{\frac{n}{1-n}} \tag{A6}$$

Equations (A5) and (A6) necessarily contain the so far undetermined mixing length "ℓ" for which either the Prandtl mixing length law

$$\ell = k\,y \tag{A7}$$

or the von Karman mixing length law

$$\ell = k\,\frac{\frac{du}{dy}}{\frac{d^2u}{dy^2}} \tag{A8}$$

may be used.

3. It is evident therefore, that the assumptions used to obtain equations (A5) and (A6) together with the mixing length laws given in equations (A7) and (A8) will yield four equations for the thickness ratio of the laminar sublayer. These are tabulated below:

Assumption	Mixing length law	Laminar sublayer thickness ratio
Equation (A5)	Prandtl (Eq. A7)	$\frac{\delta_L}{\delta} = \left[\frac{n(r-1)}{k^2\,Re_\delta}\right]^{\frac{n}{n+1}}$
	von Karman (Eq. A8)	$\frac{\delta_L}{\delta} = \left[\frac{n(r-1)}{k^2\,Re_\delta}\right]^{\frac{n}{n+1}}\left[\frac{1-n}{n}\right]^{\frac{2n}{n+1}}$
Equation (A6)	Prandtl (Eq. A7)	$\frac{\delta_L}{\delta} = \left[\frac{n^2}{k^2\,Re_\delta}\right]^{\frac{n}{n+1}}$
	von Karman (Eq. A8)	$\frac{\delta_L}{\delta} = \left[\frac{n^2}{k^2\,Re_\delta}\right]^{\frac{n}{n+1}}\left[\frac{1-n}{n}\right]^{\frac{2n}{n+1}}$

The local skin friction coefficient for incompressible flow may be calculated using the substitutions

$$\tau_w = \frac{u_L}{\delta_L}$$

$$\frac{u_L}{U_\infty} = \left(\frac{\delta_L}{\delta}\right)^{\frac{1}{n}}$$

and

$$c_f = \frac{2\tau_w}{\rho_\infty U_\infty^2}$$

together with each of the equations for the laminar sublayer thickness ratio. These are tabulated below.

Assumption	Mixing length law	Local skin friction coefficient law
Equation (A5)	Prandtl (Eq. A7)	$c_{f_i} = 2\left[\frac{n(r-1)}{k^2}\right]^{\frac{1}{1+n}}\left[\frac{1}{Re_\delta}\right]^{\frac{2}{n+1}}$ (A9)
	von Karman (Eq. A8)	$c_{f_i} = 2\left[\frac{n(r-1)}{k^2}\right]^{\frac{1-n}{1+n}}\left[\frac{1}{Re_\delta}\right]^{\frac{2}{n+1}}\left[\frac{1-n}{n}\right]^{\frac{2(1-n)}{1+n}}$ (A10)
Equation (A6)	Prandtl (Eq. A7)	$c_{f_i} = 2\left[\frac{n^2}{k^2}\right]^{\frac{1-n}{1+n}}\left[\frac{1}{Re_\delta}\right]^{\frac{2}{n+1}}$ (A11)
	von Karman (Eq. A8)	$c_{f_i} = 2\left[\frac{n^2}{k^2}\right]^{\frac{1-n}{1+n}}\left[\frac{1}{Re_\delta}\right]^{\frac{2}{n+1}}\left[\frac{1-n}{n}\right]^{\frac{2(1-n)}{1+n}}$ (A12)

APPENDIX B

Derivation of Local Skin Friction Coefficient Law for Compressible Turbulent Boundary Layers

1. It has been shown that equation (4) was the most suitable for incompressible turbulent boundary layers. This law is given as

$$c_{f_i} = 2\left[20n\right]^{\frac{1-n}{1+n}}\left[\frac{1}{Re_\delta}\right]^{\frac{2}{n+1}} \tag{4}$$

To extend this relation to compressible flows the property values (density and viscosity) need be evaluated at the edge of the laminar sublayer. Equation (4) may be written in the form

$$\frac{\tau_w}{\rho_\infty u_\infty^2} = \left[20n\right]^{\frac{1-n}{1+n}}\left[\frac{\mu_\infty}{\rho_\infty u_\infty \delta}\right]^{\frac{2}{n+1}}\left[\frac{\nu_L}{\nu_\infty}\right]^{\frac{2}{n+1}}\left[\frac{\rho_L}{\rho_\infty}\right] \tag{B1}$$

using the following substitutions

$$\frac{\rho_L}{\rho_\infty} = \frac{T_\infty}{T_L}$$

and

$$\frac{\mu_L}{\mu_\infty} = \left[\frac{T_L}{T_\infty}\right]^\omega$$

in equation (B1), yields the following relationship:

$$c_f = 2\left[20n\right]^{\frac{1-n}{1+n}}\left[\frac{1}{Re_\delta}\right]^{\frac{2}{n+1}}\left[\frac{T_\infty}{T_L}\right]^{\frac{n-2\omega-1}{n+1}} \tag{B2}$$

2. To evaluate $\frac{T_\infty}{T_L}$ it will be assumed that the Crocco quadratic form for the temperature distribution given as

$$T = A + B\left[\frac{u}{u_\infty}\right] + C\left[\frac{u}{u_\infty}\right]^2 \tag{B3}$$

is valid By evaluating equation (B3) with the usual boundary conditions, the following equation results

$$\frac{T_L}{T_\omega} = \frac{Tw}{T\infty} - \left[\frac{T_w - T_e}{T\infty}\right]\left[\frac{u_L}{u\infty}\right] - \left[\frac{T_e - T\infty}{T\infty}\right]\left[\frac{u_L}{u\infty}\right]^2 \qquad \text{(B4)}$$

3. Equation (B4) may also be written as

$$\frac{T_L}{T\infty} = 1 + r.f. \frac{\gamma-1}{2} M_\infty^2 \left[1 - \left(\frac{u_L}{u\infty}\right)^2\right] + \frac{T_w - T_e}{T\infty}\left[1 - \frac{u_L}{u\infty}\right] \qquad \text{(B5)}$$

with the velocity ratio at the edge of the laminar sublayer given as

$$\frac{u_L}{u\infty} = \left|\frac{20n}{Re_\delta}\right|^{\frac{1}{n+1}} \left\{1 + r,f, \frac{\gamma-1}{2} M_\infty^2 \left[1 - \left(\frac{u_L}{u\infty}\right)^2\right] + \frac{T_w - T_e}{T\infty}\left[1 - \frac{u_L}{u\infty}\right]\right\}^{\frac{\omega+1}{n+1}} \qquad \text{(B6)}$$

4. For all calculations using equations (B2), (B5) and (B6) ω has been taken as 0.76 and the value of r.f. as 0.896.

APPENDIX C

Derivation of Local and Average Skin Friction Coefficient Laws Based on Re_x

1. For incompressible flow the momentum equation for the boundary layer in the absence of a pressure gradient is

$$\frac{d\theta}{dx} = \frac{c_f}{2} \tag{C1}$$

or

$$\frac{dRe_\theta}{dRe_x} = \frac{c_f}{2} \tag{C2}$$

The following relation results when the right hand side of equation (4) is inserted into equation (C2);

$$\frac{dRe_\theta}{dRe_x} = \left[20n\right]^{\frac{1-n}{1+n}} \left[\frac{1}{Re_\theta}\right]^{\frac{2}{n+1}} \left[\frac{n}{(n+1)(n+2)}\right]^{\frac{2}{n+1}} \tag{C3}$$

and the substitution $\frac{\delta}{\theta} = \frac{(n+1)(n+2)}{n}$ is used.

Equation (C3) can be integrated by assuming that n is a constant along a given plate (or θ is constant). Whether or not this is a valid assumption will be verified by a comparison between the von Karman incompressible mean skin friction law and the derived relationship. Integrating equation (C3) yields

$$(Re_\theta)^{\frac{n+3}{n+1}} = \frac{n+3}{n+1} \left[\frac{1}{20n}\right]^{\frac{n-1}{n+1}} \left[\frac{n}{(n+1)(n+2)}\right]^{\frac{2}{n+1}} Re_x \tag{C4}$$

and since

$$\frac{C_{Fi}}{2} = \frac{Re_\theta}{Re_x} \tag{C5}$$

equation (C4) can be manipulated to yield

$$\frac{C_{Fi}}{2} = \left\{ \left[\frac{n+3}{n+1}\right] \left[\frac{1}{20n}\right]^{\frac{n-1}{n+1}} \left[\frac{n}{(n+1)(n+2)}\right]^{\frac{2}{n+1}} \right\}^{\frac{n+1}{n+3}} \left[\frac{1}{Re_x}\right]^{\frac{2}{n+3}} \qquad (C6)$$

A comparison between the values of C_{Fi} obtained from equation (C6) (using the n values associated with the Re_θ values of figure 3 and equation (C4)) and the values of C_{Fi} from the von Karman mean skin friction equation for incompressible flow

$$\frac{0.242}{\sqrt{C_{Fi}}} = \text{Log}_{10} \left[C_{Fi}\, Re_x\right] \qquad (C7)$$

indicated that over the Reynolds number (Re_x) range from 0.5×10^6 to 60×10^6 the agreement between C_{Fi} values is within 4 percent. This result means that at least for incompressible flow the assumption that n is a constant along a plate can only lead to small errors in the estimation of skin friction values.

Using this information, the incompressible law for local skin friction coefficients on a Re_x basis may then be derived. The momentum equation can be written as

$$\frac{d\delta}{dx} = \frac{\delta}{2\theta} C_f \qquad (C8)$$

Substituting equation (4) yields

$$\frac{d\delta}{dx} = \frac{\delta}{2\theta} \left[20n\right]^{\frac{1-n}{1+n}} \left[\frac{1}{Re_\theta}\right]^{\frac{2}{n+1}} \left[\frac{n}{(n+1)(n+2)}\right]^{\frac{2}{n+1}} \qquad (C9)$$

which may be integrated to yield the following relation

$$\frac{Re_\delta}{Re_x} = \left[\frac{n+3}{n+1}\left(\frac{\delta}{\theta}\right)\right]^{\frac{n+1}{n+3}} \left[\frac{1}{20n}\right]^{\frac{n-1}{n+3}} \left[\frac{1}{Re_x}\right]^{\frac{2}{n+3}} \qquad (C10)$$

By inserting equation (C10) into equation (C3) the following local skin friction law results

$$\frac{c_{fi}}{2} = \left[\frac{1}{20n}\right]^{\frac{n-1}{n+3}} \left[\frac{n+1}{n+3}\left(\frac{\theta}{\delta}\right)\right]^{\frac{2}{n+3}} \left[\frac{1}{Re_x}\right]^{\frac{2}{n+3}} \qquad (C11)$$

or

$$\frac{c_{fi}}{2} = \left[\frac{1}{20n}\right]^{\frac{n-1}{n+3}} \left[\frac{n}{(n+2)(n+3)}\right]^{\frac{2}{n+3}} \left[\frac{1}{Re_x}\right]^{\frac{2}{n+3}} \qquad (C12)$$

2. For compressible flow the extension of the foregoing expressions for the mean and local skin friction coefficients to compressible flows necessitates the use of an additional approximation the accuracy of which is checked with the available experimental data.

The local skin friction law (equation B2)

$$\frac{c_f}{2} = \left[\frac{1}{20n}\right]^{\frac{n-1}{n+1}} \left[\frac{1}{Re_\delta}\right]^{\frac{2}{n+1}} \left[\frac{T_\infty}{T_L}\right]^{\frac{n-2.52}{n+1}} \qquad (B2)$$

embodies the term $\left(\frac{T_\infty}{T_L}\right)$ which cannot be a predetermined constant because it depends on Reynolds number as can be seen in the following equations:

$$\frac{T_L}{T_\infty} = 1 + r.f.\ \frac{\gamma-1}{2} M_\infty^2 \left[1 - \left(\frac{u_L}{u_\infty}\right)^2\right] + \frac{T_w - T_e}{T_\infty}\left[1 - \frac{u_L}{u_\infty}\right] \qquad (C13)$$

where

$$\frac{u_L}{u_\infty} = \left[\frac{20n}{Re_\delta}\right]^{\frac{1}{n+1}} \left[\frac{T_L}{T_\infty}\right]^{\frac{1.76}{n+1}} \qquad \begin{matrix}(B6)\\ \text{or}\\ (C14)\end{matrix}$$

However, if $\frac{T_\infty}{T_L}$ is assumed to be a constant that is associated with an average value of Reynolds number, the results that are obtained may be of sufficient accuracy for most applications. This is a logical step because for a given Mach number and heat transfer rate $\frac{u_L}{u_\infty}$ is not seriously dependent

on Re_δ or Re_x. Using this assumption, the following relations may be derived from an integration of equation (B2).

$$\frac{C_F}{2} = \left\{ \left[\frac{n+3}{n+1}\right]^{n+1} \left[\frac{1}{20n}\right]^{n-1} \left[\frac{\theta}{\delta}\right]^2 \left[\frac{T_\infty}{T_L}\right]^{n-2.52} \left[\frac{1}{\overline{Re_x}}\right]^2 \right\}^{\frac{1}{n+3}} \quad \text{(C15)}$$

and

$$Re_\delta = \left[\overline{Re_x}\right]^{\frac{n+1}{n+3}} \left[\left(\frac{\delta}{\theta}\right)^{n+1} \left(\frac{n+3}{n+1}\right)^{n+1} \left(\frac{1}{20n}\right)^{n-1} \left(\frac{T_\omega}{T_L}\right)^{n-2.52}\right]^{\frac{1}{n+3}} \quad \text{(C16)}$$

where $\overline{Re_x}$ is given by

$$\overline{Re_x} = \tfrac{1}{2}\, Re_x \text{ (maximum)}$$

To determine local skin friction coefficients with the knowlege of only values of Re_x it is necessary to have available the variation of n with Re_x and Re_δ for use in equation (C16). A calculation of the variation of n with Re_x and Re_δ has been carried out for the zero heat transfer case and the results are plotted in figures 12 and 13 respectively. These calculations were made using the results tabulated in Table I, figure 3, and equations (C13) and C14). Curves similar to those shown in figures 12 and 13 may be prepared for different heat transfer rates by the same method.

Using the data plotted in figures 12 and 13 the procedure for calculating C_f as a function of Re_x is as follows:

1. Determine the maximum value of Re_x to be encounted for a given problem. The selection of this value determines n, Re_δ, and Re_x.

2. Solve equation (C16) for $\frac{T_\infty}{T_L}$.

3. Insert the values of $\frac{T_\infty}{T_L}$, n, and Re_δ in equation (B2) and solve for C_f.

By a similar procedure equation (C15) may be used to calculate mean skin friction coefficients.

As a check on the approximate analysis described above, the variation of c_f/c_{fi} with Mach number has been carried out for three values of $\overline{Re_x}$ sufficient to encompass the Re_x range of the available experimental data. Figure 14 shows the

results of these calculations compared to the available experimental data. The good agreement between theory and experiment tends to justify the approximations made in the preceding analysis.

Figure 15 shows the variation of the skin friction ratio with Mach number for a number of constant values of wall to free stream temperature ratio and a constant value of Re_x of 10^7. The similarity between curves of this figure and the results plotted in figure 8 is apparent. However, differences in the curve shapes and corresponding values of the skin friction ratio can be seen by careful examination.

TABLE I

VARIATION OF DISPLACEMENT THICKNESS RATIO, $\frac{\delta^*}{\delta}$, MOMENTUM THICKNESS RATIO, $\frac{\theta}{\delta}$, AND BOUNDARY LAYER SHAPE PARAMETER WITH MACH NUMBER, M_∞, AND HEAT TRANSFER PARAMETER, $\frac{T_w - T_c}{T_\infty}$, FOR A VELOCITY PROFILE EXPONENT, n, OF 5.0						VARIATION OF DISPLACEMENT THICKNESS RATIO, $\frac{\delta^*}{\delta}$, MOMENTUM THICKNESS RATIO, $\frac{\theta}{\delta}$, AND BOUNDARY LAYER SHAPE PARAMETER WITH MACH NUMBER, M_∞, AND HEAT TRANSFER PARAMETER, $\frac{T_w - T_c}{T_\infty}$, FOR A VELOCITY PROFILE EXPONENT, n, OF 7.0					
n	$\frac{T_w - T_c}{T_\infty}$	M_∞	$\frac{\delta^*}{\delta}$	$\frac{\theta}{\delta}$	H	n	$\frac{T_w - T_c}{T_\infty}$	M_∞	$\frac{\delta^*}{\delta}$	$\frac{\theta}{\delta}$	H
5.0	0	0	0.10741	0.11882	1.40845	7.0	0	0	0.12869	0.09781	1.29574
		2.0	0.26470	0.08266	3.07252			2.0	0.22779	0.07861	2.89785
		4.0	0.40891	0.05842	7.99213			4.0	0.35999	0.05227	7.65257
		6.0	0.80324	0.03746	16.10281			6.0	0.53914	0.03478	15.49583
		8.0	0.69592	0.02843	27.36833			8.0	0.63887	0.02618	26.44484
		10.0	0.75980	0.01816	41.83921			10.0	0.71002	0.01756	40.43280
		12.0	0.80518	0.01354	59.46824			12.0	0.76187	0.01324	57.54532
		14.0	0.83844	0.01044	80.30651			14.0	0.80058	0.01029	77.80349
		16.0	0.86347	0.00838	104.28744			16.0	0.83012	0.00831	101.10840
		18.0	0.88275	0.00671	131.56483			18.0	0.85310	0.00670	127.32836
		20.0	0.89787	0.00586	161.78378			20.0	0.87130	0.00586	154.70963
5.0	2.0	0	0.33149	0.08284	4.04071	7.0	2.0	0	0.28818	0.07124	3.76474
		2.0	0.39674	0.06996	5.67038			2.0	0.33018	0.06181	5.34218
		4.0	0.52041	0.04937	10.54081			4.0	0.45278	0.04563	10.05552
		6.0	0.62491	0.03378	18.61753			6.0	0.56600	0.03168	17.86310
		8.0	0.70938	0.02374	29.87784			8.0	0.65346	0.02268	28.80989
		10.0	0.76737	0.01732	44.30716			10.0	0.71881	0.01678	42.81883
		12.0	0.80976	0.01304	61.91131			12.0	0.76718	0.01281	59.88390
		14.0	0.84137	0.01017	82.73353			14.0	0.80594	0.01004	80.27988
		16.0	0.86543	0.00811	106.70777			16.0	[illegible]	0.00806	103.87643
		18.0	0.88410	0.00661	133.73189			18.0	0.85471	0.00659	129.69681
		20.0	0.89884	0.00547	164.31444			20.0	0.87349	0.00549	159.02338
5.0	4.0	0	0.45494	0.06438	6.58968	7.0	4.0	0	0.39698	0.05765	6.18081
		2.0	0.46907	0.05708	8.21829			2.0	0.40004	0.05164	7.74583
		4.0	0.56127	0.04297	13.06260			4.0	0.49424	0.03971	12.44883
		6.0	0.65068	0.03081	21.11632			6.0	0.58902	0.02909	20.24781
		8.0	0.72130	0.02339	32.33980			8.0	0.66657	0.02149	31.14953
		10.0	0.77437	0.01688	46.78184			10.0	[illegible]	0.01619	45.11801
		12.0	0.81408	0.01264	64.40668			12.0	0.77208	0.01241	62.31985
		14.0	0.84417	0.00981	86.18668			14.0	0.80725	0.00979	82.48178
		16.0	0.86732	0.00784	109.53174			16.0	0.83485	0.00780	105.79914
		18.0	0.88542	0.00649	136.42827			18.0	0.85638	0.00648	132.14506
		20.0	0.89978	0.00540	166.62963			20.0	0.87359	0.00541	161.47674
5.0	6.0	0	0.48867	0.05356	9.12005	7.0	6.0	0	0.41899	0.04888	8.56997
		2.0	0.49137	0.04855	10.73944			2.0	0.48231	0.04464	10.15117
		4.0	0.59382	0.03815	15.56780			4.0	0.52808	0.03545	14.81968
		6.0	0.68930	0.02838	23.98014			6.0	0.60905	0.02694	22.60958
		8.0	0.75210	0.02101	34.84831			8.0	0.67880	0.02028	33.80617
		10.0	0.78087	0.01585	49.28414			10.0	0.73373	0.01548	47.48967
		12.0	0.81818	0.01284	66.84641			12.0	0.77679	0.01203	64.87190
		14.0	0.84685	0.00967	87.58014			14.0	0.81036	0.00957	84.68130
		16.0	0.86914	0.00779	111.56611			16.0	0.83679	0.00776	107.83905
		18.0	0.88670	0.00639	138.76389			18.0	0.85780	0.00639	134.24100
		20.0	0.90070	0.00533	168.96687			20.0	0.87488	0.00534	163.80180
5.0	8.0	0	0.53907	0.04806	11.63411	7.0	8.0	0	0.46868	0.04388	10.84785
		2.0	0.54148	0.04349	13.24140			2.0	0.48388	0.03947	12.80570
		4.0	0.62063	0.03438	18.05701			4.0	0.55653	0.03220	17.28810
		6.0	0.68561	0.02629	26.07836			6.0	0.62671	0.02511	24.95819
		8.0	0.74190	0.01989	37.30018			8.0	0.68727	0.01983	34.67709
		10.0	0.78692	0.01522	51.70171			10.0	0.74060	0.01486	49.83849
		12.0	0.82206	0.01186	69.31703			12.0	0.78126	0.01166	66.99318
		14.0	0.84943	0.00943	90.07433			14.0	0.81339	0.00934	87.00779
		16.0	0.87091	0.00763	114.14155			16.0	0.83888	0.00761	110.23653
		18.0	0.88784	0.00624	141.18057			18.0	0.85859	0.00619	136.01307
		20.0	0.90160	0.00528	171.40684			20.0	0.87577	0.00527	166.19596
5.0	10.0	0	0.57288	0.04066	14.18818	7.0	10.0	0	0.49898	0.03798	13.31469
		2.0	0.58199	0.03776	15.72093			2.0	0.52739	0.03446	14.97088
		4.0	0.64388	0.03183	20.53948			4.0	0.58048	0.02972	19.83938
		6.0	0.70001	0.02481	28.89877			6.0	0.64243	0.02383	27.30132
		8.0	0.75085	0.01888	39.77225			8.0	0.69938	0.01832	38.17686
		10.0	0.79258	0.01463	54.17635			10.0	0.74704	0.01432	52.16480
		12.0	0.82574	0.01150	71.80000			12.0	0.78852	0.01135	69.20705
		14.0	0.85190	0.00920	92.59783			14.0	0.81828	0.00913	89.49854
		16.0	0.87281	0.00749	116.50800			16.0	0.84090	0.00747	112.17028
		18.0	0.88918	0.00619	143.66106			18.0	0.86073	0.00620	138.87938
		20.0	0.90248	0.00519	173.89518			20.0	0.87683	0.00521	168.29178

TABLE I (CONTINUED)

VARIATION OF DISPLACEMENT THICKNESS RATIO, $\frac{\delta^*}{\delta}$, MOMENTUM THICKNESS RATIO, $\frac{\theta}{\delta}$, AND BOUNDARY LAYER SHAPE PARAMETER WITH MACH NUMBER, M, AND HEAT TRANSFER PARAMETER, $\frac{T_w - T_R}{T_{\infty}}$, FOR A VELOCITY PROFILE EXPONENT, n, OF 9.0

n	$\frac{T_w - T_o}{T_{\infty}}$	M_{∞}	$\frac{\delta^*}{\delta}$	$\frac{\theta}{\delta}$	H
9.0	0	0	0.10083	0.06106	1.82071
		2.0	0.10941	0.06803	1.78877
		4.0	0.13180	0.08714	1.68865
		6.0	0.16992	0.09831	1.72849
		8.0	0.19384	0.09289	1.81838
		10.0	0.20011	0.01686	1.88868
		12.0	0.73864	0.01285	1.84914
		14.0	0.76030	0.01007	1.81893
		16.0	0.80132	0.00808	1.79078
		18.0	0.82784	0.00662	1.86486
		20.0	0.84790	0.00551	1.83368
9.0	2.0	0	0.89979	0.06865	1.80830
		2.0	0.38380	0.09107	1.15326
		4.0	0.40277	0.04117	1.78302
		6.0	0.41716	0.02561	17.46707
		8.0	0.60851	0.02158	28.19741
		10.0	0.67021	0.01617	41.94187
		12.0	0.73137	0.01248	58.73898
		14.0	0.77307	0.00983	78.84837
		16.0	0.80390	0.00798	101.80583
		18.0	0.82905	0.00658	127.16258
		20.0	0.84921	0.00544	156.10294
9.0	4.0	0	0.39789	0.05184	5.03943
		2.0	0.38034	0.04665	7.47705
		4.0	0.44377	0.03671	12.08935
		6.0	0.84077	0.00736	19.76606
		8.0	0.68236	0.02048	30.47892
		10.0	0.66670	0.01583	44.21764
		12.0	0.73470	0.01207	61.03563
		14.0	0.77568	0.00980	80.80206
		16.0	0.80638	0.00778	102.65039
		18.0	0.83068	0.00641	129.60096
		20.0	0.85049	0.00537	158.37989
9.0	6.0	0	0.39826	0.04468	8.98418
		2.0	0.40137	0.04108	9.76547
		4.0	0.47778	0.03221	14.38428
		6.0	0.58148	0.02847	22.04884
		8.0	0.63500	0.01939	32.74884
		10.0	0.67483	0.01484	46.49284
		12.0	0.74188	0.01173	63.24888
		14.0	0.77917	0.00937	83.19908
		16.0	0.80879	0.00765	105.73548
		18.0	0.83284	0.00631	131.93344
		20.0	0.85175	0.00529	161.05079
9.0	8.0	0	0.41848	0.05037	10.58378
		2.0	0.44839	0.03860	12.00743
		4.0	0.50680	0.03037	16.67784
		6.0	0.57980	0.02384	24.32466
		8.0	0.64660	0.01848	35.02708
		10.0	0.70207	0.01460	48.75894
		12.0	0.74878	0.01139	65.68629
		14.0	0.78281	0.00917	85.33261
		16.0	0.81113	0.00750	108.14667
		18.0	0.83432	0.00622	134.11576
		20.0	0.85298	0.00522	163.40998
9.0	10.0	0	0.43398	0.05534	12.84380
		2.0	0.47659	0.03315	14.37104
		4.0	0.53172	0.02803	18.95449
		6.0	0.59838	0.02243	26.69135
		8.0	0.65728	0.01743	37.68304
		10.0	0.70907	0.01380	51.01439
		12.0	0.75144	0.01108	67.82491
		14.0	0.78573	0.00897	87.59197
		16.0	0.81340	0.00734	110.51630
		18.0	0.83595	0.00611	136.86215
		20.0	0.85417	0.00517	165.77244

VARIATION OF DISPLACEMENT THICKNESS RATIO, $\frac{\delta^*}{\delta}$, MOMENTUM THICKNESS RATIO, $\frac{\theta}{\delta}$, AND BOUNDARY LAYER SHAPE PARAMETER WITH MACH NUMBER, M, AND HEAT TRANSFER PARAMETER, $\frac{T_w - T_R}{T_{\infty}}$, FOR A VELOCITY PROFILE EXPONENT, n, OF 11.0

n	$\frac{T_w - T_o}{T_{\infty}}$	M_{∞}	$\frac{\delta^*}{\delta}$	$\frac{\theta}{\delta}$	H
11.0	0	0	0.09371	0.07048	1.18888
		2.0	0.10388	0.08994	1.73273
		4.0	0.31498	0.04280	7.33333
		6.0	0.43038	0.03018	14.26388
		8.0	0.55837	0.02171	25.84348
		10.0	0.63437	0.01618	39.20890
		12.0	0.69416	0.01244	55.80386
		14.0	0.74006	0.00981	75.44343
		16.0	0.77584	0.00798	97.98455
		18.0	0.80416	0.00658	122.78308
		20.0	0.82648	0.00542	152.36458
11.0	2.0	0	0.10188	0.05877	3.80186
		2.0	0.34951	0.04981	5.02933
		4.0	0.36388	0.03789	9.60148
		6.0	0.47758	0.02777	17.19448
		8.0	0.57105	0.02084	27.40428
		10.0	0.64381	0.01554	41.42801
		12.0	0.70028	0.01207	58.01988
		14.0	0.74411	0.00959	77.58134
		16.0	0.77864	[illegible]	[illegible]
		18.0	0.80614	[illegible]	[illegible]
		20.0	0.82829	0.00540	153.38889
11.0	4.0	0	0.37171	0.04708	5.78868
		2.0	0.31847	0.04879	7.30311
		4.0	0.40308	0.03106	11.88948
		6.0	0.50138	0.02288	19.43411
		8.0	0.58535	0.01949	30.03992
		10.0	0.65283	[illegible]	[illegible]
		12.0	0.70604	[illegible]	[illegible]
		14.0	0.74801	0.00936	79.91453
		16.0	0.78134	0.00762	102.53281
		18.0	0.80806	0.00631	128.04656
		20.0	0.82970	0.00529	156.84310
11.0	6.0	0	0.38943	0.04099	9.04398
		2.0	0.36180	0.03784	9.56131
		4.0	0.43758	0.03101	14.11186
		6.0	0.53248	0.02410	22.09038
		8.0	0.59846	0.01854	32.28158
		10.0	0.66119	0.01441	45.88480
		12.0	0.71188	0.01139	62.47388
		14.0	0.75178	0.00918	82.07434
		16.0	0.78398	0.00749	104.67280
		18.0	0.80994	0.00622	130.30900
		20.0	0.83107	0.00523	158.91013
11.0	8.0	0	0.37540	0.03846	10.29022
		2.0	0.40208	0.03403	11.81404
		4.0	0.46633	0.02852	16.34993
		6.0	0.54122	0.02286	23.80459
		8.0	0.61052	0.01770	34.49153
		10.0	0.66904	0.01382	48.08036
		12.0	0.71880	0.01110	64.57958
		14.0	0.75538	0.00898	84.32804
		16.0	0.78850	0.00738	106.88141
		18.0	0.81178	0.00613	132.41067
		20.0	0.83241	0.00517	161.00580
11.0	10.0	0	0.41330	0.03297	12.53584
		2.0	0.43581	0.03102	14.04000
		4.0	0.49137	0.02643	18.59251
		6.0	0.55816	0.02135	26.14520
		8.0	0.62166	0.01693	36.72180
		10.0	0.67648	0.01344	50.33482
		12.0	0.72182	0.01079	[illegible]
		14.0	0.75884	0.00877	[illegible]
		16.0	0.78898	0.00724	[illegible]
		18.0	0.81356	0.00604	[illegible]
		20.0	0.83371	0.00512	[illegible]

TABLE I (CONTINUED)

VARIATION OF DISPLACEMENT THICKNESS RATIO, $\frac{\delta^*}{\delta}$, MOMENTUM THICKNESS RATIO, $\frac{\theta}{\delta}$, AND BOUNDARY LAYER SHAPE PARAMETER WITH MACH NUMBER, M, AND HEAT TRANSFER PARAMETER, $\frac{T_w - T_R}{T_{t_\infty}}$, FOR A VELOCITY PROFILE EXPONENT, n, OF 5.0

n	$\frac{T_w - T_\infty}{T_{t_\infty}}$	M_∞	$\frac{\delta^*}{\delta}$	$\frac{\theta}{\delta}$	H
5.0	-2.0	4.0	0.39183	0.07235	5.38766
		6.0	0.57218	0.04215	13.57533
		8.0	0.69086	0.02735	24.89580
		10.0	0.75152	0.01909	39.37140
		12.0	0.80032	0.01404	57.00142
		14.0	0.83937	0.01074	77.78399
		16.0	0.86144	0.00847	101.70012
		18.0	0.88135	0.00684	128.83985
		20.0	0.89888	0.00563	159.30726
5.0	-4.0	6.0	0.63330	0.04843	11.01383
		8.0	0.68386	0.02986	22.37894
		10.0	0.74283	0.02013	36.89031
		12.0	0.79515	0.01457	54.57720
		14.0	0.83210	0.01105	75.31222
		16.0	0.85934	0.00865	99.24104
		18.0	0.87892	0.00695	126.60432
		20.0	0.89587	0.00571	156.90018
5.0	-6.0	6.0	0.68265	0.04734	14.41234
		8.0	0.64340	0.02242	19.85411
		10.0	0.73240	0.02131	34.36761
		12.0	0.78963	0.01516	52.08443
		14.0	0.82879	0.01137	72.89358
		16.0	0.85716	0.00884	96.96833
		18.0	0.87844	0.00708	124.06780
		20.0	0.89493	0.00580	154.27586
5.0	-8.0	8.0	0.62047	0.04543	17.31749
		10.0	0.72106	0.02263	31.90455
		12.0	0.78372	0.01580	49.60127
		14.0	0.82525	0.01172	70.41909
		16.0	0.85480	0.00905	94.46409
		18.0	0.87691	0.00721	121.62275
		20.0	0.89377	0.00588	152.00680
5.0	-10.0	8.0	0.59244	0.04019	14.73999
		10.0	0.70091	0.02416	29.01328
		12.0	0.77738	0.01650	47.11515
		14.0	0.82152	0.01209	67.97472
		16.0	0.85253	0.00927	91.93333
		18.0	0.87534	0.00735	119.04844
		20.0	0.89368	0.00587	149.53099

VARIATION OF DISPLACEMENT THICKNESS RATIO, $\frac{\delta^*}{\delta}$, MOMENTUM THICKNESS RATIO, $\frac{\theta}{\delta}$, AND BOUNDARY LAYER SHAPE PARAMETER WITH MACH NUMBER, M, AND HEAT TRANSFER PARAMETER, $\frac{T_w - T_R}{T_{t_\infty}}$, FOR A VELOCITY PROFILE EXPONENT, n, OF 7.0

n	$\frac{T_w - T_\infty}{T_{t_\infty}}$	M_∞	$\frac{\delta^*}{\delta}$	$\frac{\theta}{\delta}$	H
7.0	-2.0	4.0	0.38871	0.04304	9.21415
		6.0	0.50724	0.03868	13.11272
		8.0	0.62259	0.02588	24.05719
		10.0	0.70067	0.01841	38.07170
		12.0	0.75832	0.01372	55.12391
		14.0	0.80702	0.01057	75.40208
		16.0	0.82773	0.00839	98.65316
		18.0	0.85145	0.00681	125.03871
		20.0	0.87011	0.00566	153.72798
7.0	-4.0	6.0	0.68897	0.04378	10.70400
		8.0	0.80422	0.03764	21.36259
		10.0	0.69094	0.01932	35.76087
		12.0	0.75414	0.01418	52.98231
		14.0	0.79330	0.01085	73.11521
		16.0	0.82526	0.00859	96.07643
		18.0	0.84974	0.00693	122.61143
		20.0	0.86990	0.00572	151.90559
7.0	-6.0	6.0	0.61882	0.05066	8.26885
		8.0	0.58326	0.03019	19.32097
		10.0	0.[illegible]	0.02036	33.40373
		12.0	0.74414	0.01473	50.52274
		14.0	0.78940	0.01116	70.73477
		16.0	0.82270	0.00875	94.02388
		18.0	0.84789	0.00705	120.23369
		20.0	0.86706	0.00579	149.86143
7.0	-8.0	8.0	0.53900	0.03303	16.92401
		10.0	0.66824	0.02153	31.03578
		12.0	0.[illegible]2	0.01531	48.17113
		14.0	0.78532	0.01144	68.40507
		16.0	0.82005	0.00894	91.73378
		18.0	0.84619	0.00717	118.01953
		20.0	0.86619	0.00587	147.59796
7.0	-10.0	8.0	0.53041	0.03856	14.50766
		10.0	0.65536	0.02285	28.67396
		12.0	0.73040	0.01593	45.83040
		14.0	0.78104	0.01168	66.87446
		16.0	0.81779	0.00915	89.32240
		18.0	0.84433	0.00729	115.81619
		20.0	0.86509	0.00596	145.15101

TABLE I (CONCLUDED)

VARIATION OF DISPLACEMENT THICKNESS RATIO, $\frac{\delta^*}{\delta}$, MOMENTUM THICKNESS RATIO, $\frac{\theta}{\delta}$, AND BOUNDARY LAYER SHAPE PARAMETER WITH MACH NUMBER, M, AND HEAT TRANSFER PARAMETER, $\frac{T_w - T_R}{T_{(D)}}$, FOR A VELOCITY PROFILE EXPONENT, n, OF 9.0

n	$\frac{T_w - T_e}{T_{(D)}}$	$M_{(D)}$	$\frac{\delta^*}{\delta}$	$\frac{\theta}{\delta}$	H
9.0	-2.0	4.0	0.28455	0.05567	5.11227
		6.0	0.43744	0.03501	12.85475
		8.0	0.57624	0.02440	23.61885
		10.0	0.69932	0.01782	37.41771
		12.0	0.71450	0.01327	54.22005
		14.0	0.78434	0.01031	74.14161
		16.0	0.79466	0.00824	96.42991
		18.0	0.82538	0.00672	122.82738
		20.0	0.84856	0.00558	151.72043
9.0	-4.0	6.0	0.41954	0.03982	10.53491
		8.0	0.55729	0.02614	21.31982
		10.0	0.64874	0.01847	35.12182
		12.0	0.71311	0.01372	51.97522
		14.0	0.76028	0.01058	71.86200
		16.0	0.79391	0.00840	94.75000
		18.0	0.82346	0.00684	120.39474
		20.0	0.84519	0.00565	149.59292
9.0	-6.0	6.0	0.37196	0.04542	8.19022
		8.0	0.53582	0.02818	19.02699
		10.0	0.63726	0.01940	32.85052
		12.0	0.70633	0.01431	49.70443
		14.0	0.75509	0.01087	69.54922
		16.0	0.79305	0.00859	92.32829
		18.0	0.82149	0.00695	118.20144
		20.0	0.84[illegible]9	0.00572	147.51748
9.0	-8.0	8.0	0.51122	0.03089	16.71134
		10.0	0.62478	0.02044	30.56751
		12.0	0.69912	0.01478	47.39461
		14.0	0.75150	0.01117	67.27842
		16.0	0.79010	0.00877	90.09132
		18.0	0.81947	0.00705	116.24113
		20.0	0.84335	0.00580	145.24138
9.0	-10.0	8.0	0.48868	0.03384	14.38478
		10.0	0.61104	0.02181	28.27395
		12.0	0.69145	0.01528	45.13704
		14.0	0.74880	0.01148	64.98569
		16.0	0.78704	0.00896	87.83482
		18.0	0.81738	0.00718	113.84401
		20.0	0.84087	0.00580	142.52542

VARIATION OF DISPLACEMENT THICKNESS RATIO, $\frac{\delta^*}{\delta}$, MOMENTUM THICKNESS RATIO, $\frac{\theta}{\delta}$, AND BOUNDARY LAYER SHAPE PARAMETER WITH MACH NUMBER, M, AND HEAT TRANSFER PARAMETER, $\frac{T_w - T_c}{T_{(D)}}$, FOR A VELOCITY PROFILE EXPONENT, n, OF 11.0

n	$\frac{T_w - T_c}{T_{(D)}}$	$M_{(D)}$	$\frac{\delta^*}{\delta}$	$\frac{\theta}{\delta}$	H
11.0	-2.0	4.0	0.25150	0.04986	5.04412
		6.0	0.41470	0.03296	12.69172
		8.0	0.53803	0.02306	23.33044
		10.0	0.62414	0.01688	36.95086
		12.0	0.68774	0.01284	53.55919
		14.0	0.73583	0.01008	73.14115
		16.0	0.77296	0.00816	95.80571
		18.0	0.80212	0.00680	121.55030
		20.0	0.82537	0.00550	150.07273
11.0	-4.0	6.0	0.36118	0.03638	10.42100
		8.0	0.51874	0.02459	21.09394
		10.0	0.61312	0.01765	34.73654
		12.0	0.68097	0.01325	51.39623
		14.0	0.73143	0.01031	70.94083
		16.0	0.76998	0.00823	93.54018
		18.0	0.80003	0.00671	119.22504
		20.0	0.82387	0.00557	147.91741
11.0	-6.0	6.0	0.33548	0.04123	8.13738
		8.0	0.49707	0.02639	18.83668
		10.0	0.60121	0.01850	32.49730
		12.0	0.67381	0.01370	49.18248
		14.0	0.72845	0.01057	68.77010
		16.0	0.76692	0.00839	91.51551
		18.0	0.79749	0.00686	116.99413
		20.0	0.82253	0.00564	145.79787
11.0	-8.0	8.0	0.47246	0.03850	16.57898
		10.0	0.59428	0.01844	30.28235
		12.0	0.66820	0.01421	48.88248
		14.0	0.72205	0.01085	68.55300
		16.0	0.76371	0.00858	89.31739
		18.0	0.79567	0.00693	114.81862
		20.0	0.82075	0.00572	143.49650
11.0	-10.0	8.0	0.44414	0.03584	14.30735
		10.0	0.57417	0.02049	28.02343
		12.0	0.65813	0.01473	44.67783
		14.0	0.71702	0.01118	64.30493
		16.0	0.76040	0.00874	87.04238
		18.0	0.79241	0.00704	112.69888
		20.0	0.81914	0.00581	140.98107

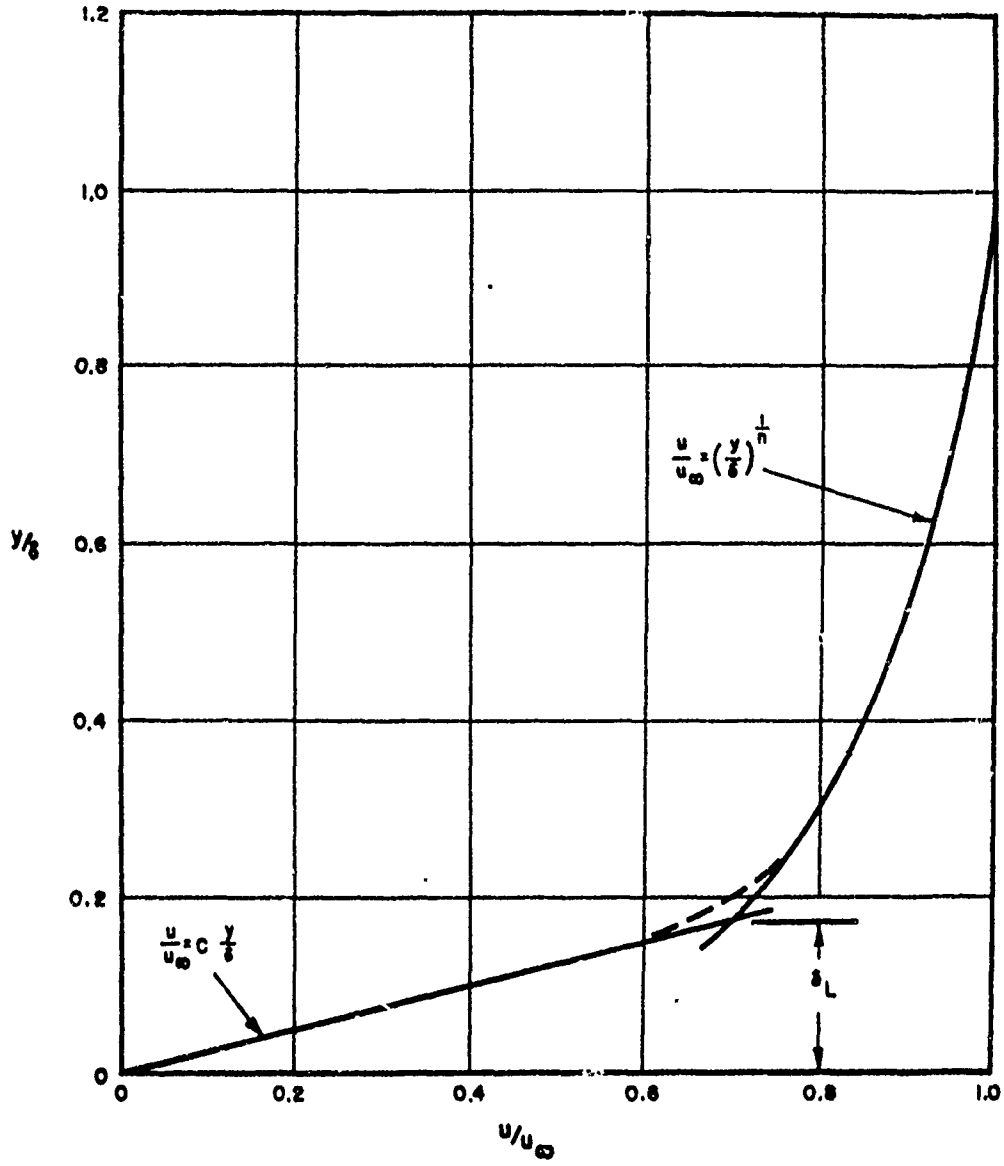

FIG. 1 VELOCITY DISTRIBUTION ACROSS A TYPICAL TURBULENT BOUNDARY LAYER

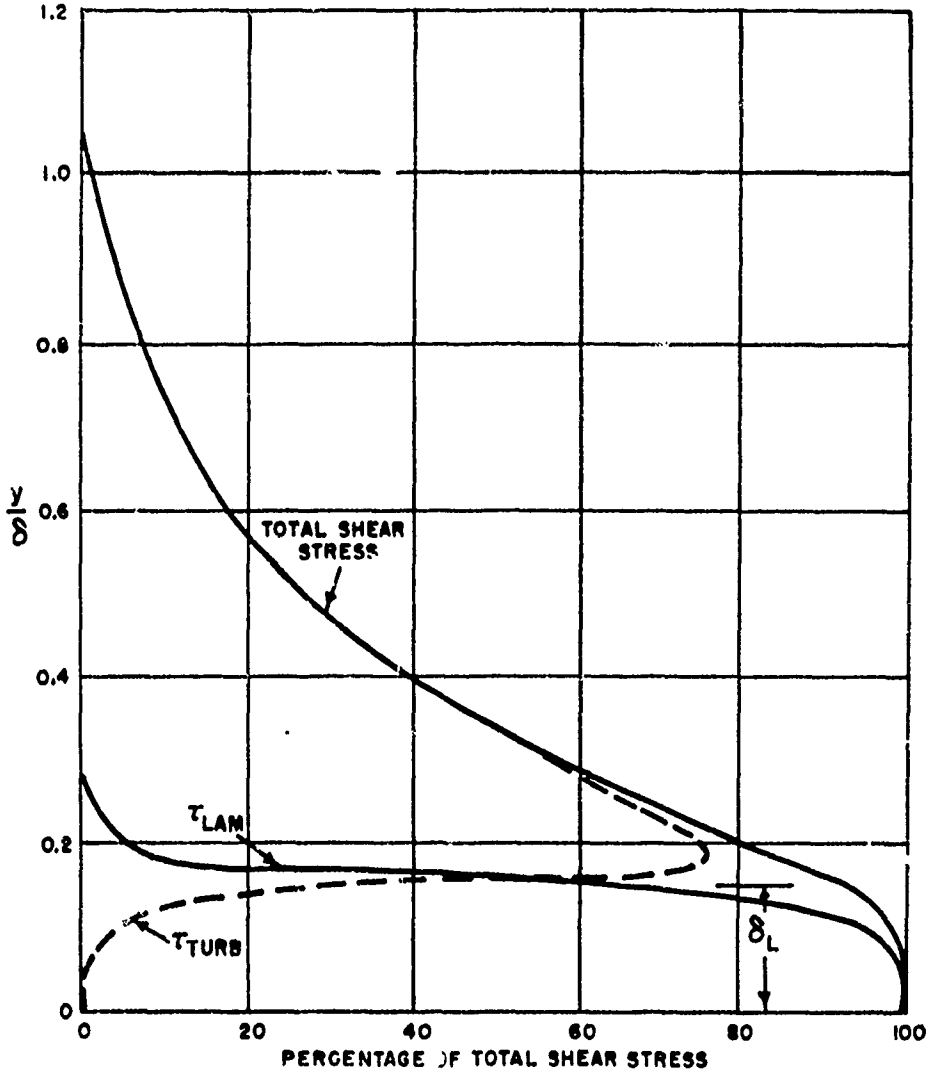

FIG. 2 SCHEMATIC VIEW OF VISCOUS AND TURBULENT SHEAR STRESS ACROSS A TYPICAL TURBULENT BOUNDARY LAYER

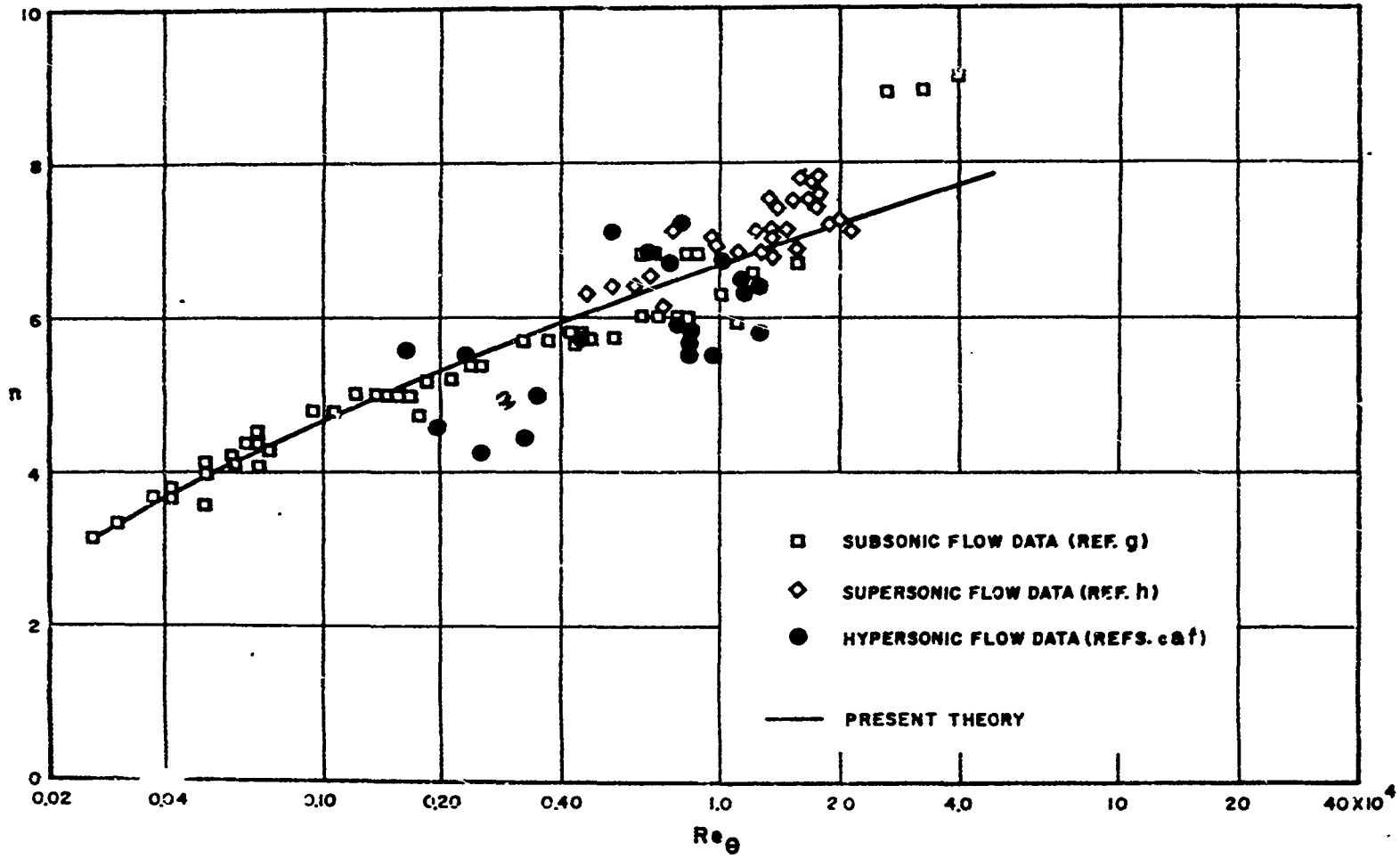

F 3.3 VARIATION OF TURBULENT BOUNDARY LAYER VELOCITY PROFILE EXPONENT (n) WITH REYNOLDS NUMBER (Re_θ)

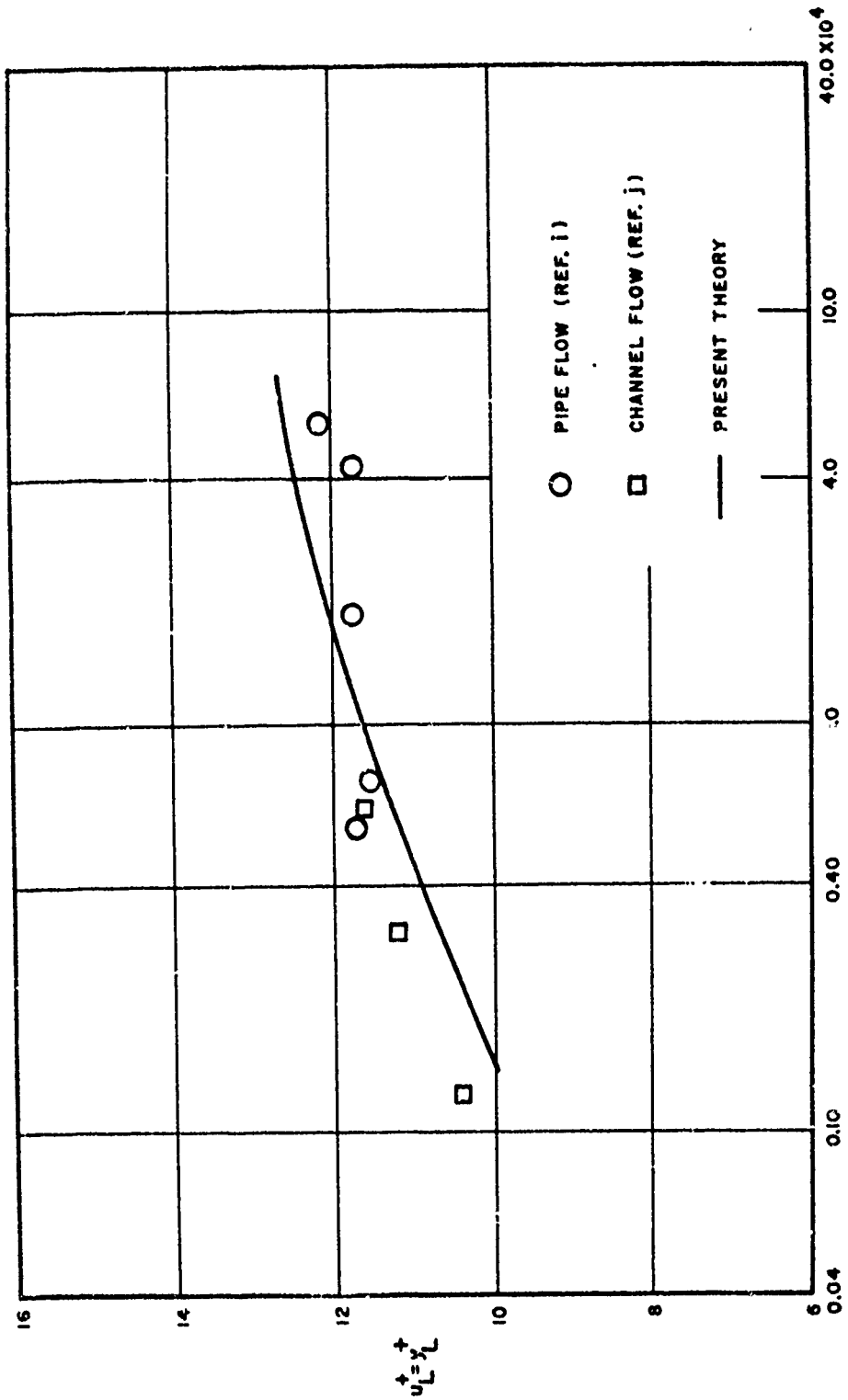

FIG. 4 VARIATION OF $u_L^+ = y_L^+$ WITH REYNOLDS NUMBER (Re_θ) FOR INCOMPRESSIBLE FLOW

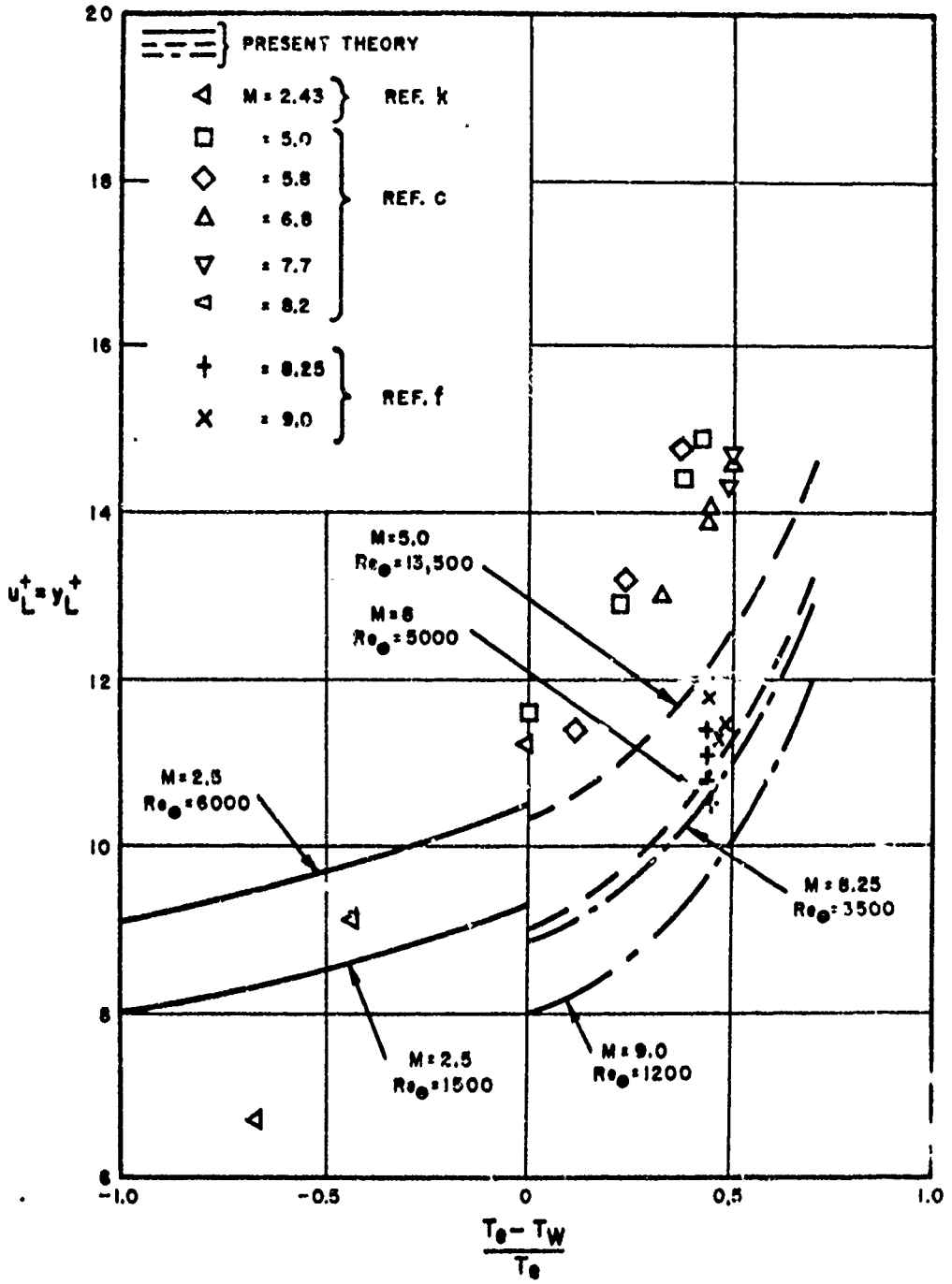

FIG. 5 COMPARISON BETWEEN THEORETICAL AND EXPERIMENTAL VALUES OF $u_L^+ = y_L^+$ FOR COMPRESSIBLE FLOW

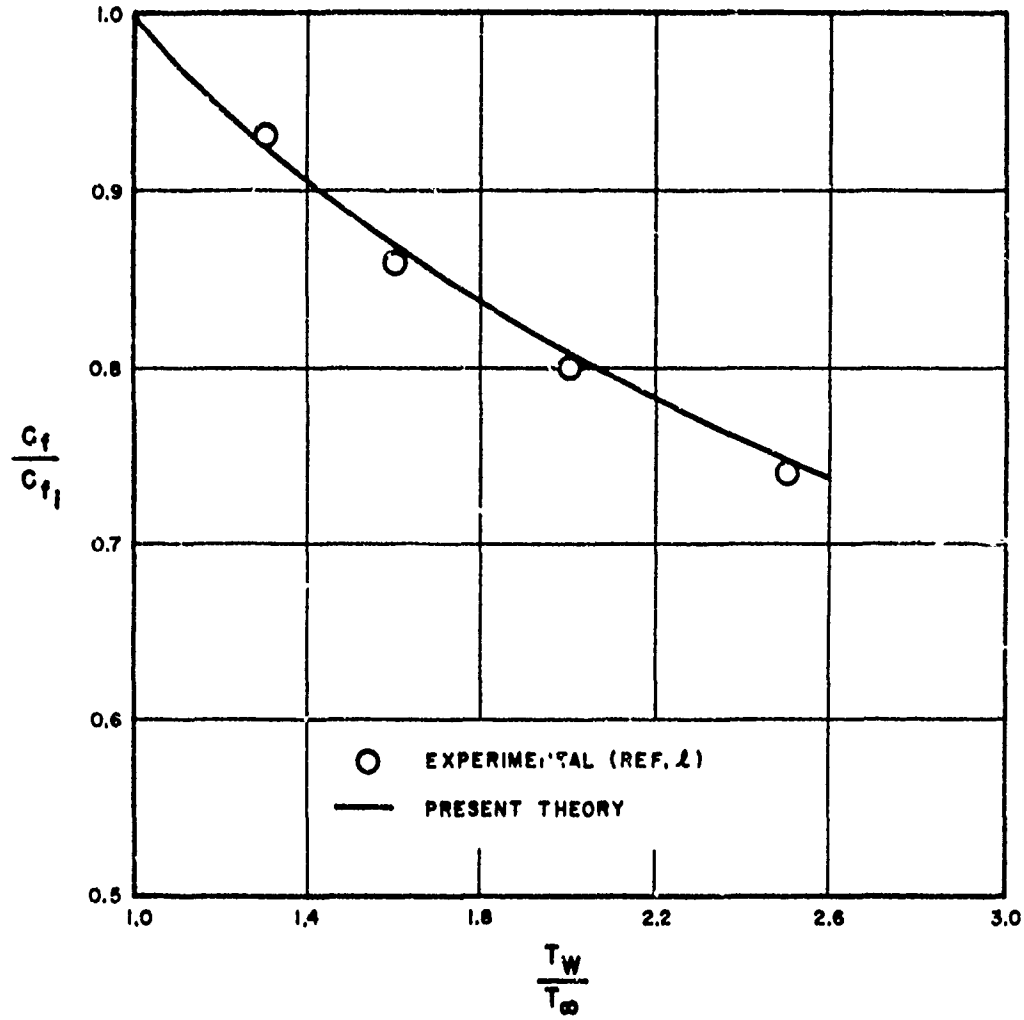

FIG. 6 INFLUENCE OF HEAT TRANSFER ON SKIN FRICTION RATIO FOR INCOMPRESSIBLE FLOW

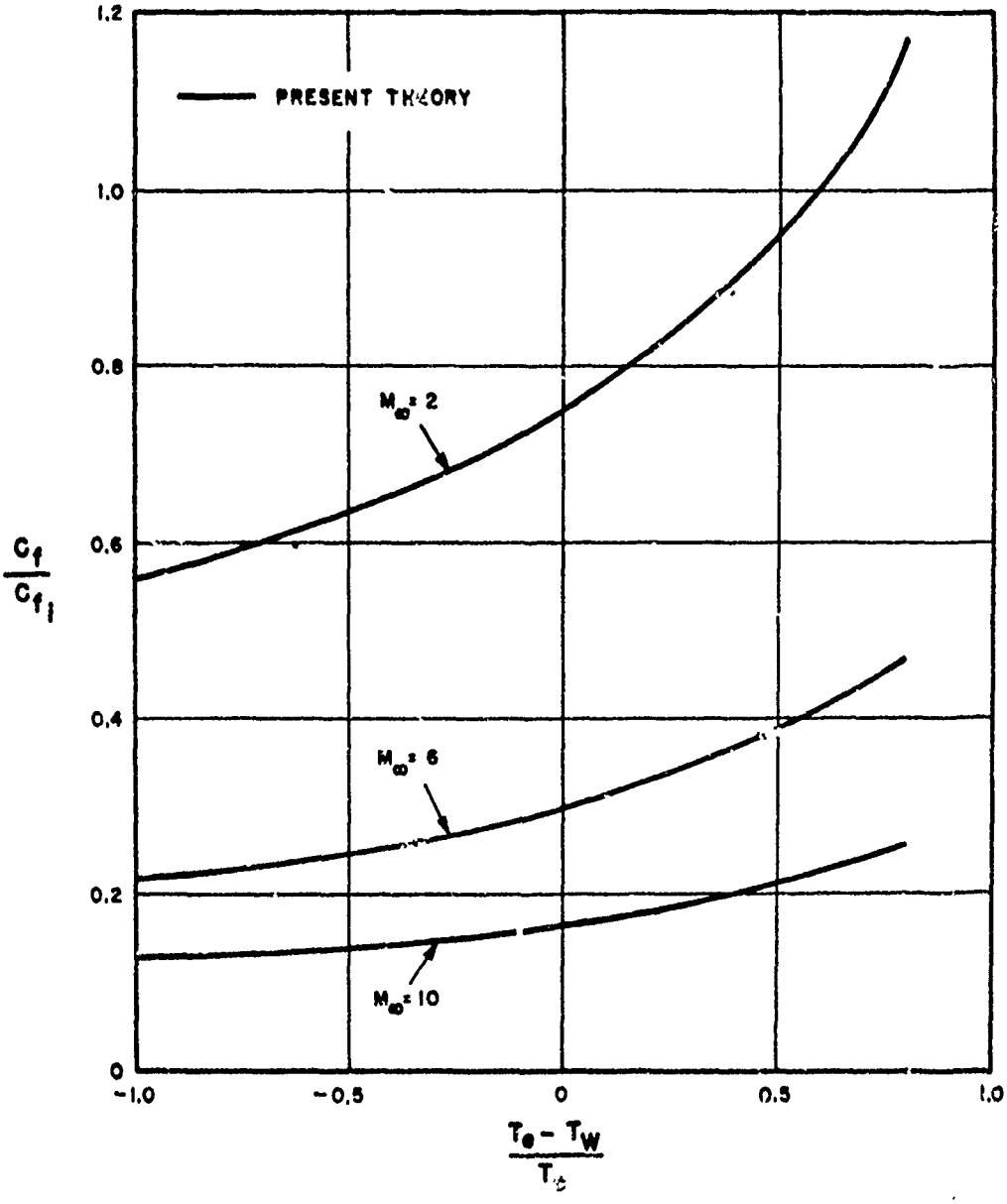

FIG. 7 INFLUENCE OF HEAT TRANSFER ON SKIN FRICTION RATIO FOR THREE VALUES OF MACH NUMBER AND Re_e =13,500

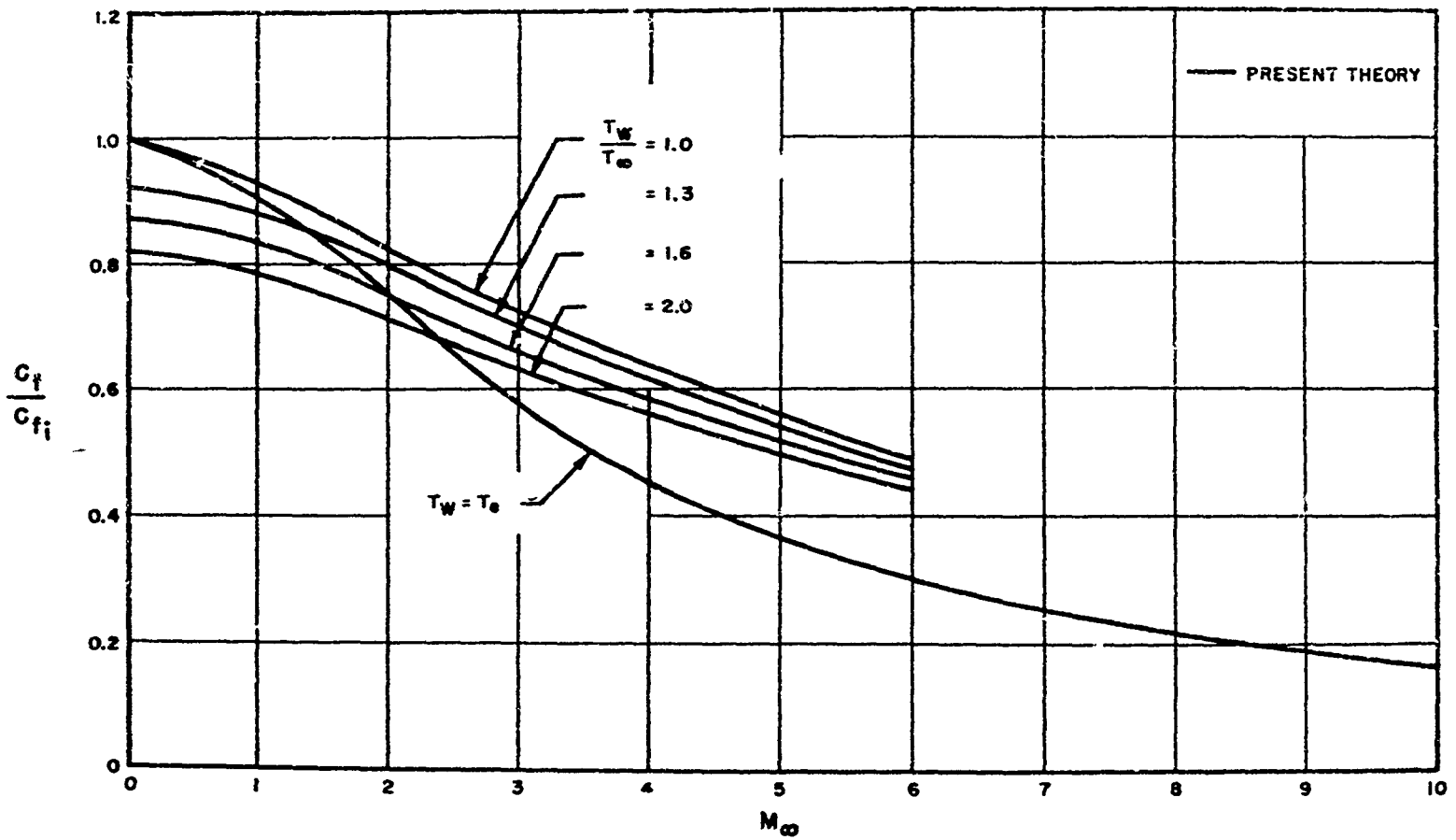

FIG. 8 VARIATION OF SKIN FRICTION RATIO WITH MACH NUMBER FOR SEVERAL CONSTANT VALUES OF WALL TO FREE STREAM TEMPERATURE RATIO AND Re_θ=13,500

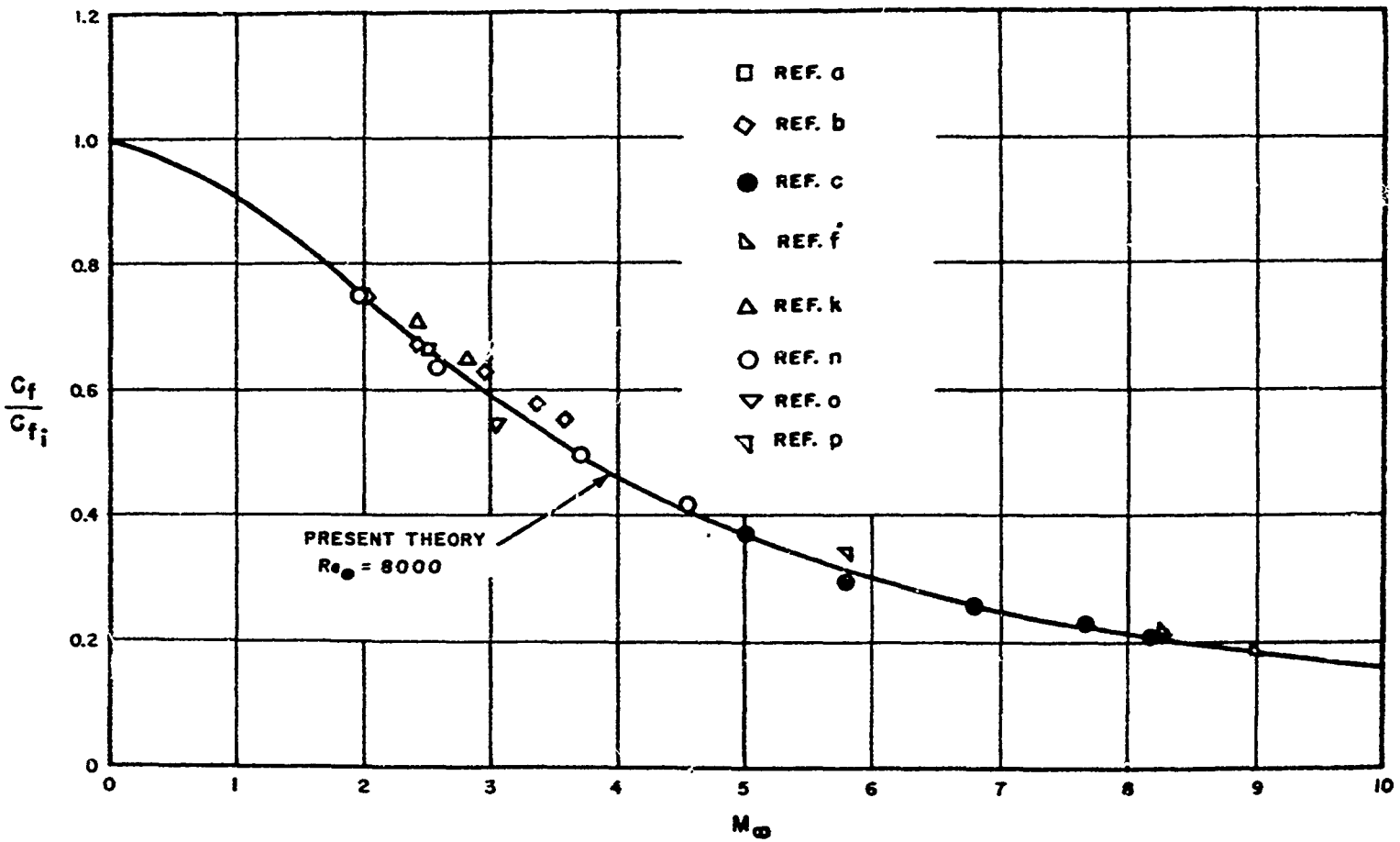

FIG. 9 VARIATION OF SKIN FRICTION RATIO WITH MACH NUMBER FOR ZERO HEAT TRANSFER AND Re_θ = 8000

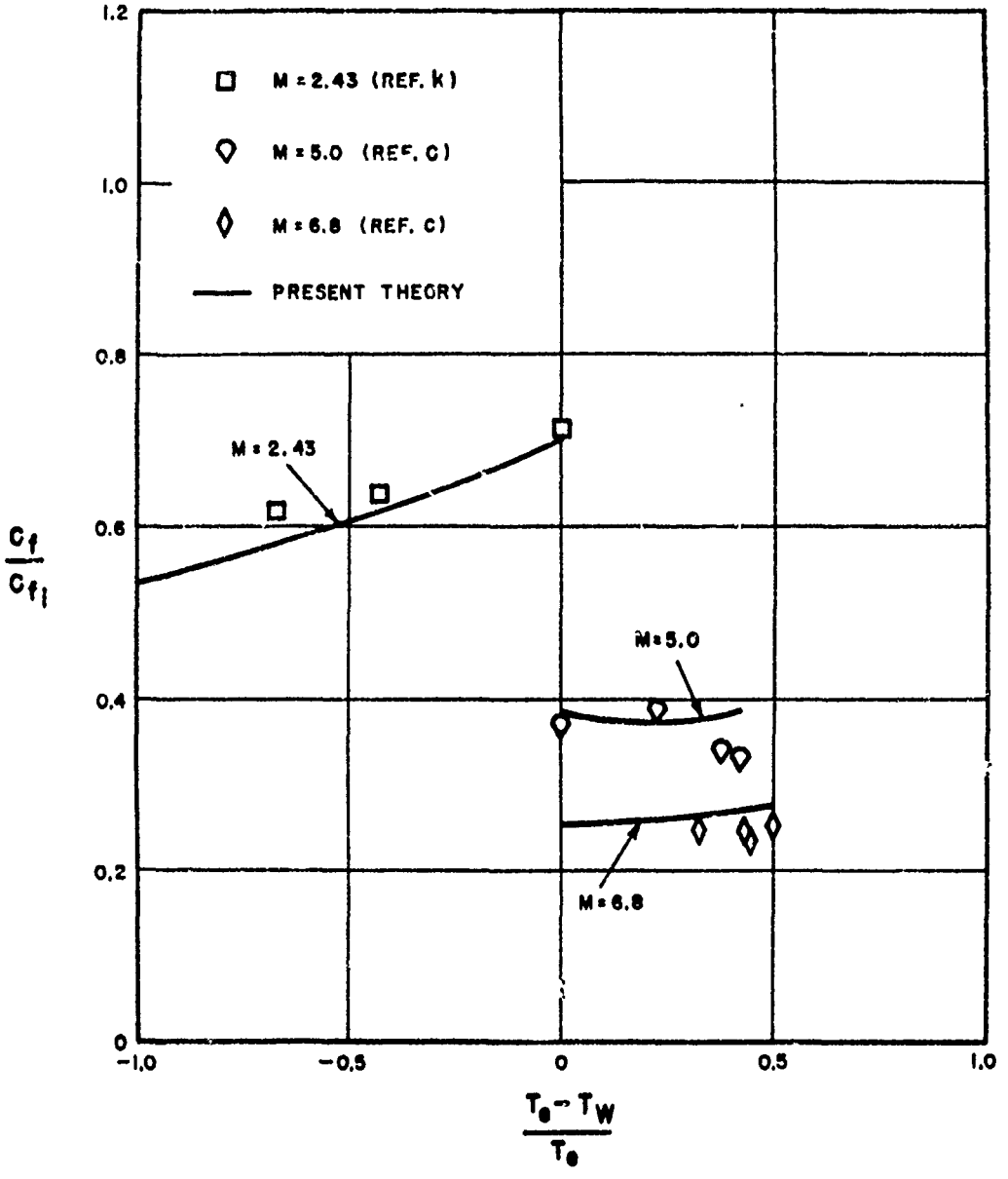

FIG. 10 COMPARISON BETWEEN THEORETICAL AND EXPERIMENTAL VALUES OF SKIN FRICTION RATIO FOR M=2.43, 5.0 AND 6.8

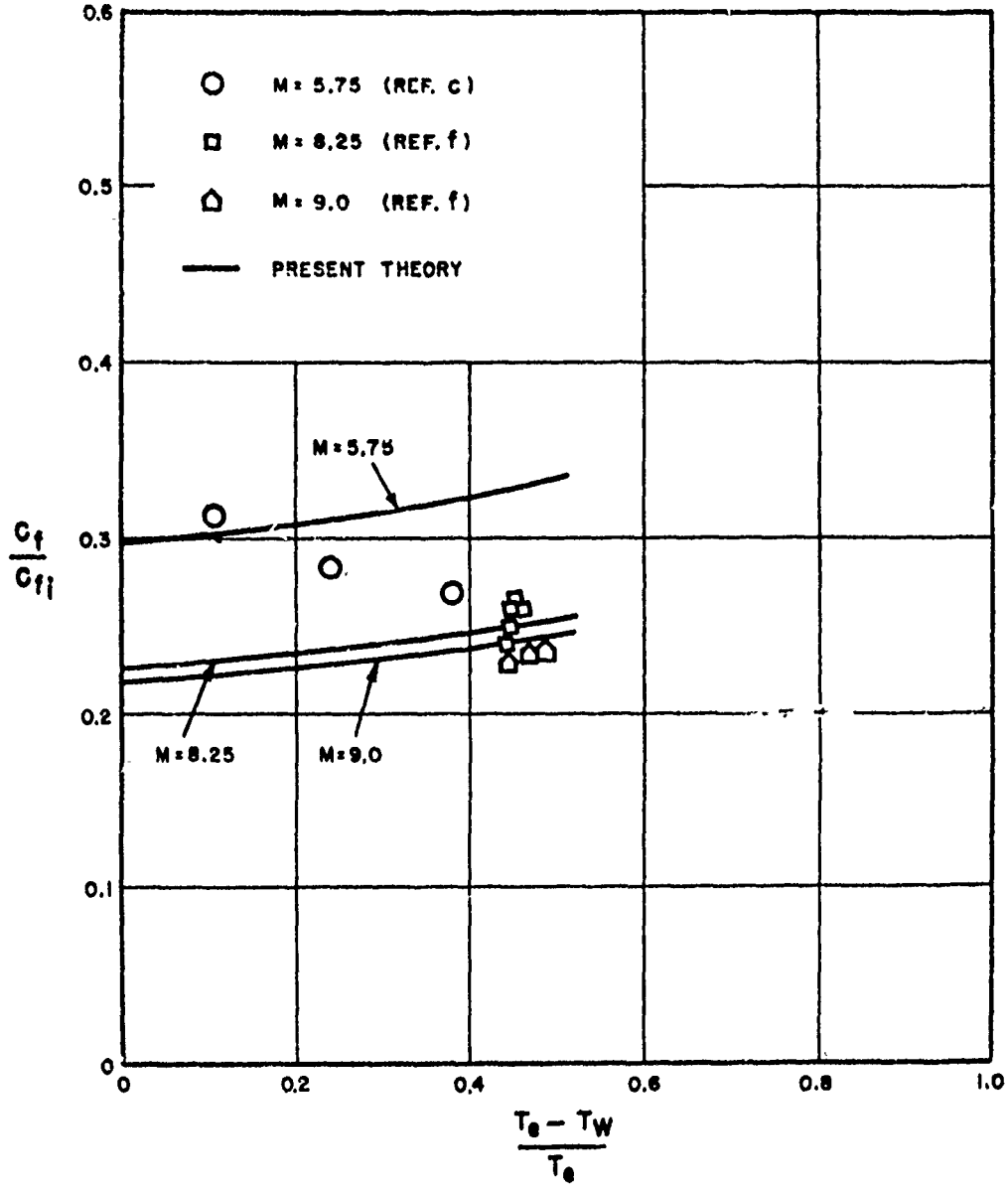

FIG. 11 COMPARISON BETWEEN THEORETICAL AND EXPERIMENTAL VALUES OF SKIN FRICTION RATIO FOR M=5.75, 8.25, AND 9.0

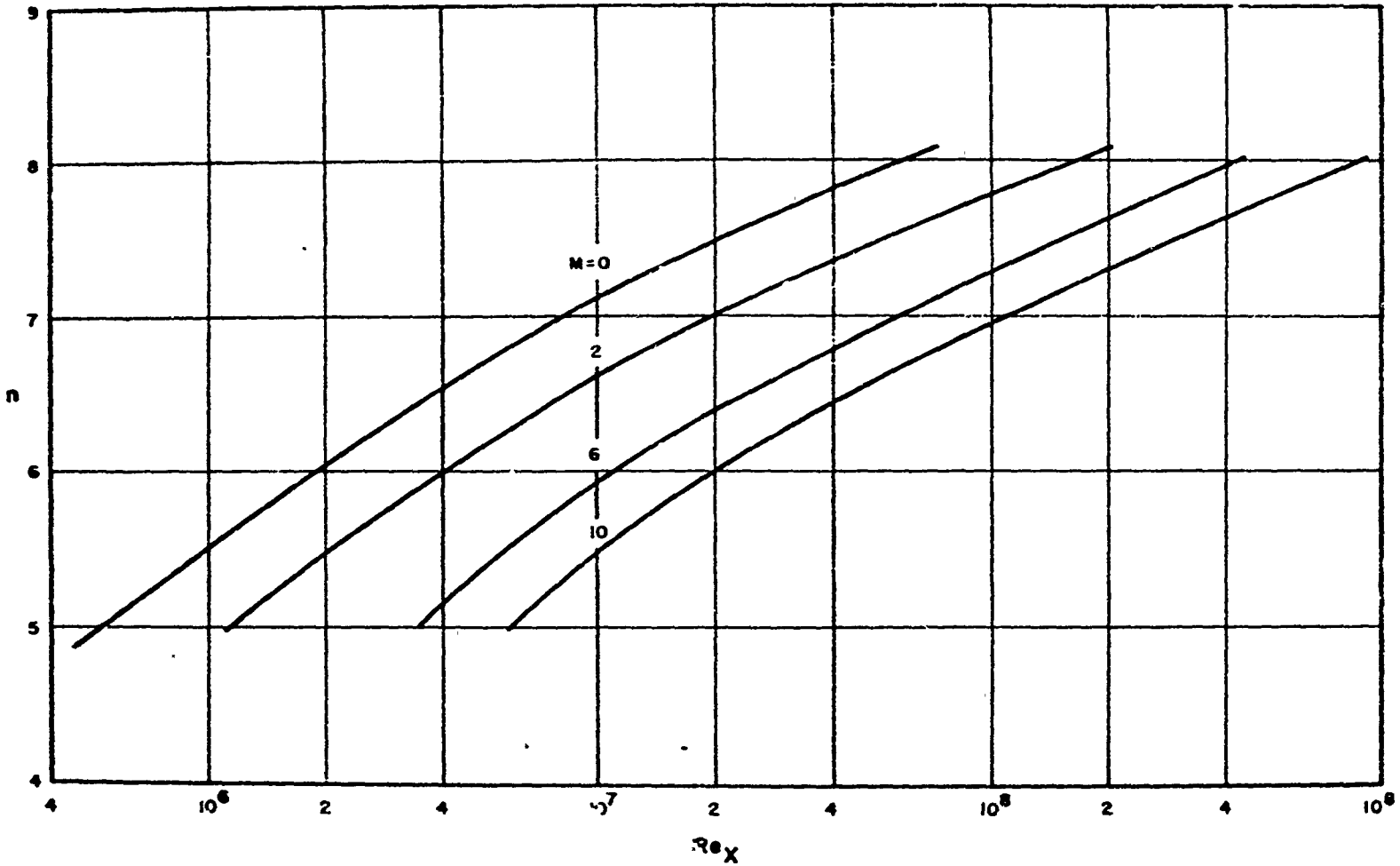

FIG.12 VARIATION OF n WITH Re_x FOR SEVERAL CONSTANT VALUES OF MACH NUMBER

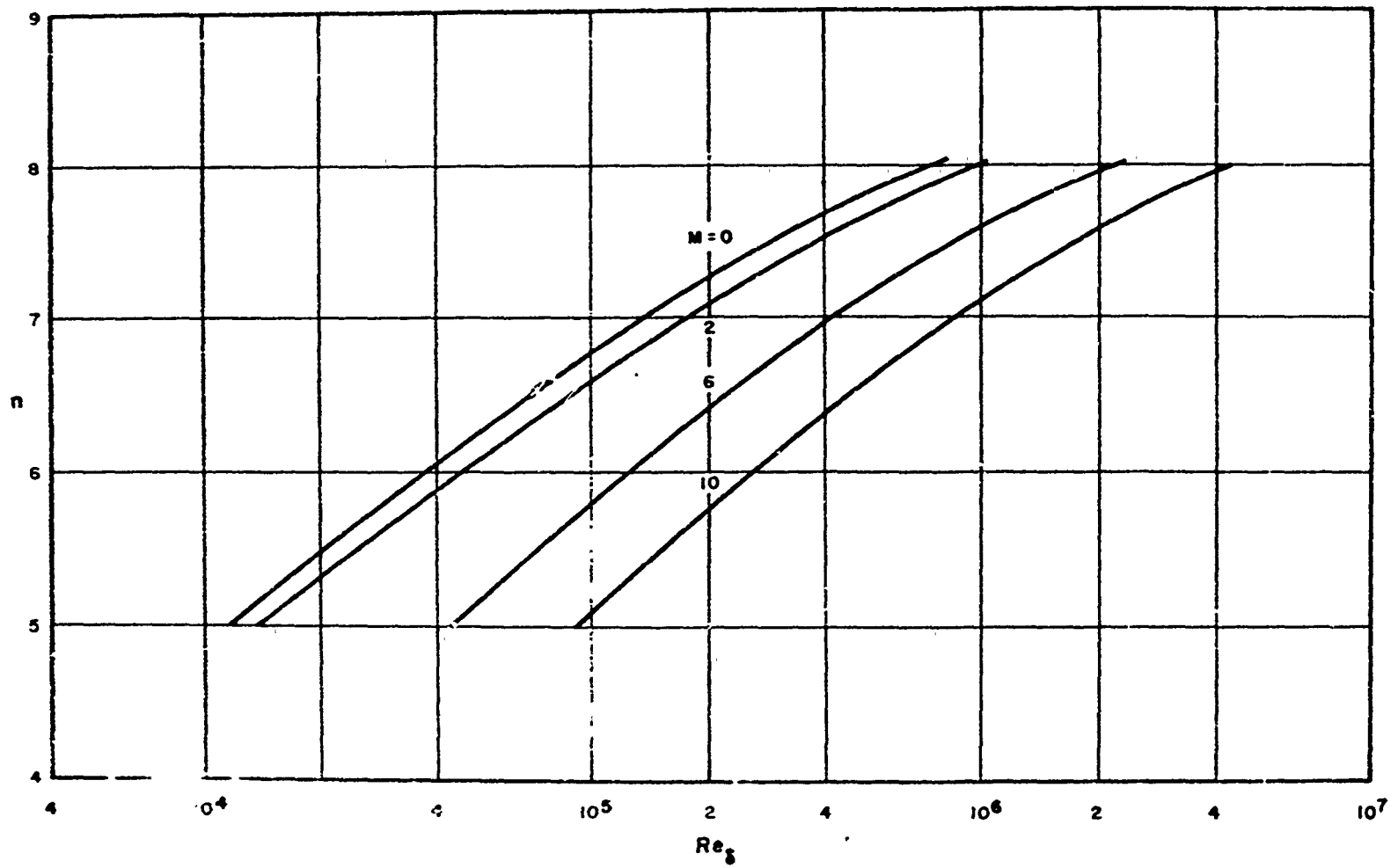

FIG. 13 VARIATION OF n WITH Re_δ FOR SEVERAL CONSTANT VALUES OF MACH NUMBER

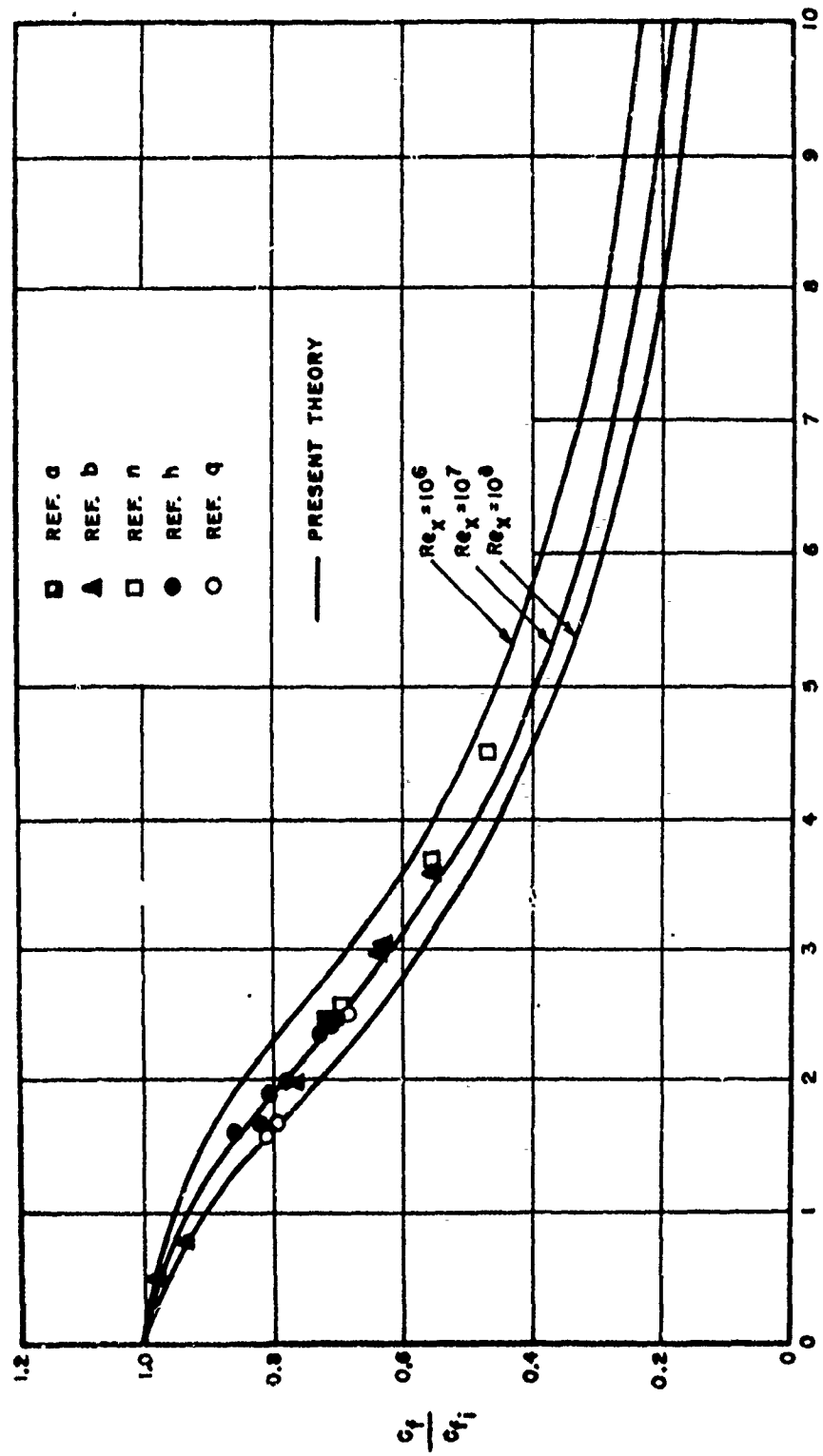

FIG. 14 VARIATION OF SKIN FRICTION RATIO WITH MACH NUMBER FOR CONSTANT VALUES OF Re_x OF 10^6, 10^7, AND 10^8

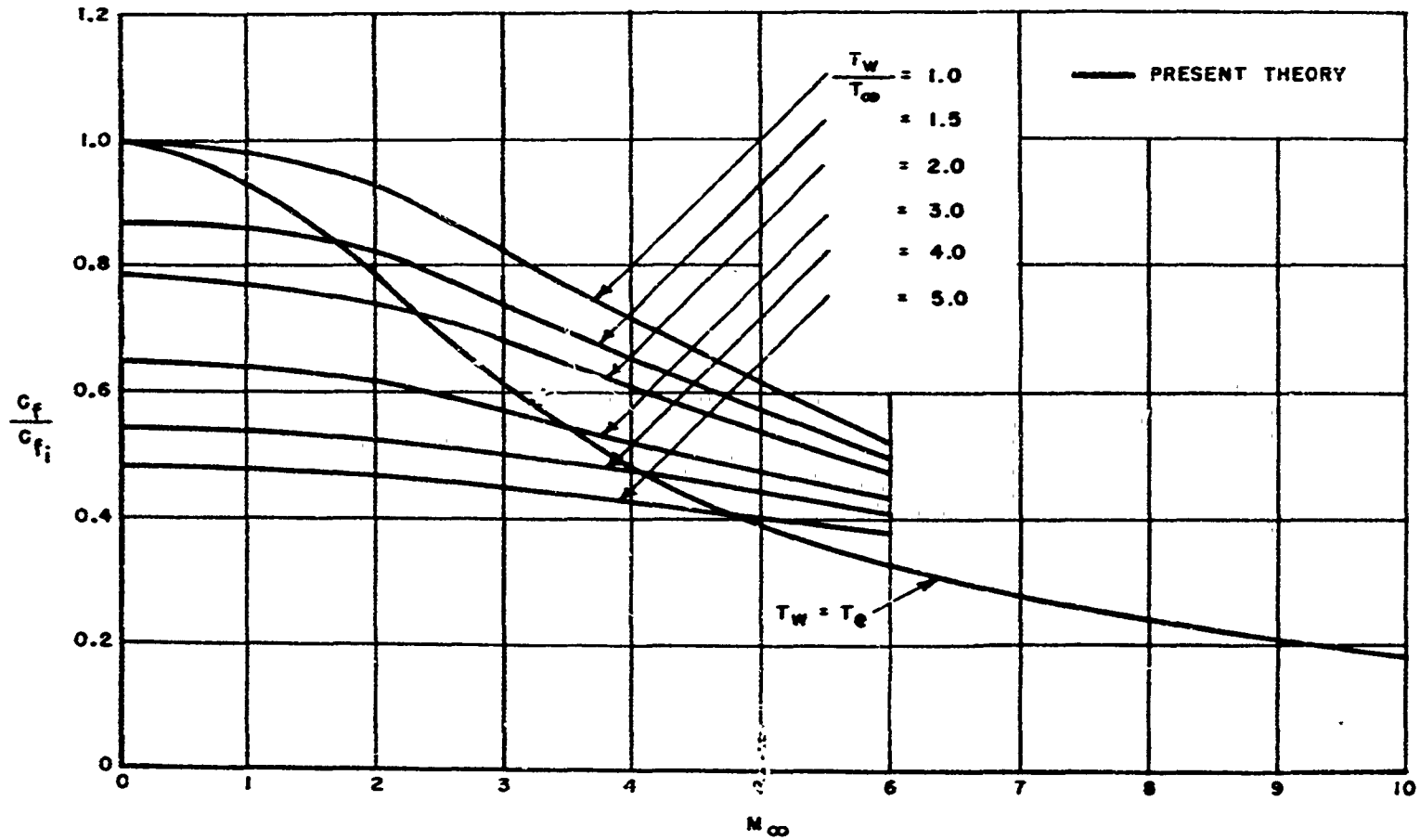

FIG. 15 VARIATION OF SKIN FRICTION RATIO WITH MACH NUMBER FOR SEVERAL CONSTANT VALUES OF WALL TO FREE-STREAM TEMPERATURE RATIO AND A CONSTANT Re_x OF 10^7

NAVORD Report 3854

Aeroballistic Research Department
External Distribution List for Aeroballistics Research (XI)

No. of Copies	
	Chief, Bureau of Ordnance Department of the Navy Washington 25, D. C.
1	Attn: Re3d
2	Attn: Re6
2	Attn: Re9a
	Chief, Bureau of Aeronautics Department of the Navy Washington 25, D. C.
1	Attn: AER-TD-414
2	Attn: RS-7
	Commander U. S. Naval Ordnance Test Station Inyokern P. O. China Lake, California
2	Attn: Technical Library
1	Attn: Code 5003
	Commander U. S. Naval Air Missile Test Center Point Mugu, California
2	Attn: Technical Library
	Superintendent U. S. Naval Postgraduate School Monterey, California
1	Attn: Librarian
	Commanding Officer and Director David Taylor Model Basin Washington 7, D. C.
2	Attn: Hydrodynamics Laboratory
	Chief of Naval Research Library of Congress Washington 25, D. C.
2	Attn: Technical Info. Div.
	Office of Naval Research Department of the Navy Washington 25, D. C.
1	Attn: Code 438
2	Attn: Code 463

No. of Copies	
	National Bureau of Standards Washington 25, D. C.
1	Attn: Nat'l Applied Math. Lab.
1	Attn: Librarian (Ord. Dev. Div.)
1	Attn: Chief, Mechanics Div.
	National Bureau of Standards Corona Laboratories (Ord. Dev. Div.) Corona, California
1	Attn: Dr. H. Thomas
	University of California 211 Mechanics Building Berkeley 4, California
1	Attn: Mr. G. J. Maslach
1	Attn: Dr. S. A. Schaaf
2	Commanding General Redstone Arsenal Huntsville, Alabama Attn: Tech. Library
1	Jet Propulsion Lab. California Institute of Technology 4800 Oak Grove Drive Pasadena 3, California Attn: F. E. Goddard, Jr.
	California Institute of Technology Pasadena 4, California
2	Attn: Librarian (Guggenheim Aero Lab)
1	Attn: Dr. H. T. Nagamatsu
1	Attn: Prof. M. S. Plesset
1	Attn: Dr. Hans W. Liepmann VIA: BuAer Representative
	University of Illinois 202 E. E. R. L. Urbana, Illinois
1	Attn: Prof. A. H. Taub
1	Director Inst. for Fluid Dynamics and Applied Math University of Maryland College Park, Maryland
	Massachusetts Inst. of Technology Cambridge 39, Massachusetts
1	Attn: Prof. G. Stever
1	Attn: Prof. J. Kaye

No. of Copies	
	University of Michigan Ann Arbor, Michigan
1	Attn: Prof. Otto Laporte
	University of Michigan Willow Run Research Center Ypsilanti, Michigan
1	Attn: L. R. Biasell
	Dept. of Mechanical Engr. University of Minnesota Institute of Technology Minneapolis 14, Minnesota
1	Attn: Prof. N. A. Hall
	The Ohio State University Columbus, Ohio
2	Attn: G. L. Von Eschen
	Polytechnic Institute of Brooklyn Aerodynamics Laboratory 527 Atlantic Avenue Freeport, New York
1	Attn: Dr. Antonio Ferri VIA: ONR
	Massachusetts Inst. of Technology Cambridge 39, Massachusetts
2	Attn: Project Meteor
1	Attn: Guided Missiles Library
1	Princeton University Forrestal Research Center Library Project Squid Princeton, New Jersey
	Armour Research Foundation 35 West 33rd Street Chicago 16, Illinois
1	Attn: Engr. Mech. Div. VIA: ONR
	Princeton University Princeton, New Jersey
1	Attn: Prof. S. Bogdonoff VIA: ONR

No. of Copies	
	Applied Physics Laboratory The Johns Hopkins University 8621 Georgia Avenue Silver Spring, Maryland
1	Attn: Arthur G. Norris VIA: NIO
1	Cornell Aeronautical Lab., Inc. 4455 Genesee Street Buffalo 21, New York VIA: BuAer Rep.
1	Defense Research Laboratory University of Texas Box 1, University Station Austin, Texas
	Eastman Kodak Company 50 W. Main Street Rochester 4, New York
1	Attn: Dr. Herbert Trotter, Jr. VIA: NIO
	General Electric Company Building #1, Campbell Ave. Plant Schenectady, New York
1	Attn: Joseph C. Hoffman VIA: InsMachinery
	The Rand Corporation 1700 Main Street Santa Monica, California
1	Attn: The Librarian
	Consolidated Vultee Aircraft Corp. Daingerfield, Texas
1	Attn: J. E. Arnold VIA: Dev. Contract Office
	Douglas Aircraft Company, Inc. 3000 Ocean Park Boulevard Santa Monica, California
1	Attn: Mr. E. F. Burton VIA: BuAer Resident Rep.
1	BuAer Representative AeroJet--General Corp. 6352 North Irwindale Ave. Azusa, California

No. of Copies	
	North American Aviation, Inc. 12214 Lakewood Boulevard Downey, California
2	Attn: Aerophysics Library VIA: BuAer Representative
	United Aircraft Corporation East Hartford 8, Connecticut
1	Attn: Robert C. Sale VIA: BuAer Representative
	National Advisory Committee for Aero. 1512 H Street, Northwest Washington 25, D. C.
5	Attn: E. B. Jackson
	Ames Aeronautical Laboratory Moffett Field, California
1	Attn: H. J. Allen
2	Attn: Dr. A. C. Charters
	NACA Lewis Flight Propulsion Lab Cleveland Hopkins Airport Cleveland 11, Ohio
1	Attn: John C. Evvard
	Langley Aeronautical Laboratory Langley Field, Virginia
1	Attn: Theoretical Aerodynamics Div.
1	Attn: J. V. Becker
1	Attn: Dr. Adolf Buseman
1	Attn: Mr. C. H. McLellan
1	Attn: Mr. J. Stack
	Harvard University 21 Vanserg Building Cambridge 38, Massachusetts
1	Attn: Prof. Carrett Birkhoff
	The Johns Hopkins University Charles and 34th Streets Baltimore 18, Maryland
1	Attn: Dr. Francis H. Clauser
	New York University 45 Fourth Avenue New York 3, New York
1	Attn: Professor R. Courant

No. of Copies

1 Dr. Allen E. Puckett, Head
Missile Aerodynamics Department
Hughes Aircraft Company
Culver City, California

1 Dr. Gordon N. Patterson, Director
Institute of Aerophysics
University of Toronto
Toronto 5, Ontario, Canada
VIA: BuOrd (Ad8)

Acroon, Inc.
385 E. Green Street
Pasadena 1, California
1 VIA: Inspector of Naval Mat'l
1206 S. Santee Street
Los Angeles 15, Calif.

Engineering Research Inst.
East Engineering Building
1 Ann Arbor, Michigan
Attn: Director of Icing Research

NAVORD Report 3854

Aeroballistic Research Department
External Distribution List for Aeroballistics Research (XIa)

No. of Copies	
6	Office of Naval Research Branch Office Navy 100 Fleet Post Office New York, New York
	Commanding General Aberdeen Proving Ground Aberdeen, Maryland
1	Attn: Dr. B. L. Hicks
	National Bureau of Standards Aerodynamics Section Washington 25, D. C.
1	Attn: Dr. G. B. Schubauer, Chief
	Ames Aeronautical Laboratory Moffett Field, California
1	Attn: Walter G. Vincenti
	University of California Observatory 21 Berkeley 4, California
1	Attn: Leland E. Cunningham
	Graduate School Aeronautical Engr. Cornell University Ithaca, New York
1	Attn: W. R. Sears, Director VIA: ONR
	Applied Math. and Statistics Lab. Stanford University Stanford, California
1	Attn: R. J. Langle, Associate Dir.
	University of Minnesota Dept. of Aeronautical Engr. Minneapolis, Minnesota
1	Attn: Professor R. Hermann
	Massachusetts Inst. of Technology Dept. of Mathematics, Room 2-270 77 Massachusetts Avenue Cambridge, Massachusetts
1	Attn: Prof. Eric Reissner

No. of Copies	
	Case Institute of Technology Dept. of Mechanical Engineering Cleveland, Ohio
1	Attn: Professor G. Kuerti VIA: ONR
	Harvard University 109 Pierce Hall Cambridge 38, Massachusetts
1	Attn: Professor R. von Mises

EXTERNAL DISTRIBUTION

No. of Copies	
1	Mr. A. I. Moskovitz Bureau of Ordnance (Re9a) Navy Department Washington, D. C.
1	Chief, Naval Operations Department of the Navy Washington 25, D. C.
1	The Artillery School Anti-aircraft & Guided Missiles Br. Fort Bliss, Texas Attn: Research & Analysis Sec.
1	Mr. Felix W. Fenter Defense Research Laboratory University of Texas Austin, Texas
1	Prof. R. F. Probstein Division of Engineering Brown University Providence, Rhode Island
1	Commander U. S. Naval Proving Ground Dahlgren, Virginia
1	Jet Propulsion Laboratory 4800 Oak Grove Drive Pasadena, California Attn: Dr. P. P. Wegener
1	Flight and Aerodynamics Laboratory Research Division Ordnance Missile Laboratory Redstone Arsenal Huntsville, Alabama Attn: J. L. Potter, Chief
5	U. S. Air Force Headquarters Arnold Engineering Development Center (ARDC) Tullahoma, Tennessee Attn: AEKS
1	Dr. R. H. Mills Wright Air Development Center Wright-Patterson Air Force Base Dayton, Ohio

No. of Copies

1 Mr. Ronald Smelt
Chief, Gas Dynamics Facility
Arnold Research Organization, Inc.
Tullahoma, Tennessee

1 Dr. Henry Nagamatsu
California Institute of Technology
Pasadena, California

1 Professor N. J. Hoff
Polytechnic Institute of Brooklyn
Brooklyn, New York

1 Dr. F. L. Wattendorf
Facilities Division DCS/Development
Hdqts. USAF, Room 5C368
Pentagon, Washington 25, D. C.

1 Professor A. Kantrowitz
Cornell University
Department of Aeronautical Engineering
Ithaca, New York

1 Professor Lester Lees
California Institute of Technology
Pasadena, California

1 Dr. H. G. Stever
MIT, Department of Aeronautical Engineering
Cambridge, Massachusetts

1 Professor G. L. Von Eschen
Aeronautical Engineering Department
Ohio State University
Columbus, Ohio

1 Mr. R. L. Bayless
Consolidated Vultee Aircraft Corporation
San Diego, California

1 Professor S. M. Bogdonoff
Department of Aeronautical Engineering
Princeton University
Princeton, New Jersey

1 Professor J. Kaye
MIT, Physics Department
Cambridge, Massachusetts

No. of Copies	
1	Dr. Ernst R. G. Eckert Department of Mechanical Engineering University of Minnesota Minneapolis 14, Minnesota
1	Mr. Mervin Sibulkin Jet Propulsion Laboratory 4800 Oak Grove Drive Pasadena, California
1	Dr. G. R. Eber Holloman Air Force Base Alamagordo, New Mexico
1	Dr. Albert E. Lombard Pentagon, Rm. 4E348 Washington, D. C.
1	Dr. E. R. Van Driest Aerophysics Laboratory North American Aviation, Inc. Downing, California
1	Dr. Paul A. Libby Polytechnic Institute of Brooklyn 99 Livingston Street Brooklyn, New York
1	Dr. W. S. Bradfield Aero. Engr. Dept. University of Minnesota Minneapolis, Minnesota
1	Dr. D. Coles California Institute of Technology Pasadena 4, California
1	Prof. Dr. H. Reichardt Max Planck Institut fuer Stroemungsforschung Goettingen, Germany
1	Prof. Dr. H. Schlichting Institut fuer Stroemungsmechanik der Technischen Hochschule Wodanstrasse 42 Braunschweig, Germany
1	Prof. Dr. J. Ackeret Soenneggstrasse 3 Zurich 6, Switzerland

No. of Copies

Director
Naval Research Laboratory
Washington 25, D. C.
1 Attn: Code 2021
1 Attn: Code 3800

Office, Chief of Ordnance
U. S. Army
Washington 25, D. C.
1 Attn: ORDTU

2 Library Branch
Research and Development Board
Pentagon 3D1041
Washington 25, D. C.

Chief, AFSWP
P. O. Box 2610
Washington 25, D. C.
1 Attn: Technical Library

1 Chief, Physical Vulnerability Branch
Air Targets Division
Directorate of Intelligence
Headquarters, USAF
Washington 25, D. C.

Commanding General
Wright Air Development Center
Wright-Patterson Air Force Base
Dayton, Ohio
5 Attn: WCACL
1 Attn: WCSD
2 Attn: WCSOR
2 Attn: WCRRN
1 Attn: WCACD
1 Attn: WCRRF
2 Attn: WCLGH

1 Director
Air University Library
Maxwell Air Force Base, Alabama

Commanding General
Aberdeen Proving Ground
Aberdeen, Maryland
1 Attn: C. L. Poor
1 Attn: D. S. Dederick

No. of Copies	
1	D. N. Morris Douglas Aircraft Company, Inc. El Segundo Division El Segundo, California
1	K. E. Van Every Douglas Aircraft Company, Inc. El Segundo Division El Segundo, California
1	Dr. G. V. Bull Canadian Armament Research and Development Establishment P. O. Box 1427 Quebec, Quebec, Canada
2	Dr. Philip A. Hufton Aeronautical Department Royal Aircraft Establishment Farnborough, England
1	Paul F. Brinich NACA, Lewis Flight Propulsion Lab Cleveland 11, Ohio
1	Dr. I. I. Glass Institute of Aerophysics University of Toronto Toronto 5, Ontario, Canada
1	Prof. H. F. Ludloff Daniel Guggenheim School of Aeronautics New York University New York 3, New York
1	John Laufer Jet Propulsion Laboratory California Institute of Technology 4800 Oak Grove Drive Pasadena 2, California
1	William H. Dorrance Consolidated Vultee Aircraft Corporation San Diego, California
1	Professor Dean MIT, Gas Turbine Laboratory Engineering Department Cambridge, Massachusetts

No. of Copies	
1	Major J. B. Robinson U. S. Air Force Main Navy Building, Rm. 3816 Washington 25, D. C.
1	D. R. Bartz Jet Propulsion Laboratory California Institute of Technology 4800 Oak Grove Drive Pasadena 3, California
1	William F. Brown Los Alamos Scientific Laboratory University of California P. O. Box 1663 Los Alamos, New Mexico
1	P. S. Klebanoff Aerodynamic Section National Bureau of Standards Washington 25, D. C.
1	Judson Baron Naval Supersonic Laboratory Massachusetts Institute of Technology Cambridge, Massachusetts
1	Marvin Sweeney, Jr. Naval Supersonic Laboratory Massachusetts Institute of Technology Cambridge, Massachusetts
1	Dr. F. Frenkiel Applied Physics Laboratory The Johns Hopkins University 8621 Georgia Avenue Silver Spring, Maryland
1	Dr. F. K. Hill Applied Physics Laboratory The Johns Hopkins University 8621 Georgia Avenue Silver Spring, Maryland
1	Mr. E. A. Bonney Applied Physics Laboratory The Johns Hopkins University 8621 Georgia Avenue Silver Spring, Maryland

No. of Copies	
1	Dr. Francis R. Hama Institute of Fluid Dynam University of Maryland College Park, Maryland
1	Prof. S. F. Shen Aeronautical Engr. Dept University of Maryland College Park, Maryland
1	Prof. S. I. Pai Institute of Fluid Dynami University of Maryland College Park, Maryland
1	Dr. William Bollay Aerophysics Development C 15304 Sunset Blvd. Pacific Palisades, Calif
1	Dr. D. R. Chapman NACA, Ames Aeronautical L Moffett Field, California
1	Alvin Seiff NACA, Ames Aeronautical L Moffett Field, California
1	Morris W. Rubesin NACA, Ames Aeronautical L Moffett Field, California
1	R. G. Deissler NACA, Lewis Flight Propul Cleveland 11, Ohio
1	Coleman Du P. Donaldson 247 Nassau Street Princeton, New Jersey
1	R. J. Monaghan Aeronautical Department Royal Aircraft Establish Farnborough, England
1	Satish Dhawan California Institute o Pasadena 4, California

REPRODUCTION QUALITY NOTICE

We use state-of-the-art high speed document scanning and reproduction equipment. In addition, we employ stringent quality control techniques at each stage of the scanning and reproduction process to ensure that our document reproduction is as true to the original as current scanning and reproduction technology allows. However, the following original document conditions may adversely affect Computer Output Microfiche (COM) and/or print reproduction:

- Pages smaller or larger than 8.5 inches x 11 inches.
- Pages with background color or light colored printing.
- Pages with smaller than 8 point type or poor printing.
- Pages with continuous tone material or color photographs.
- Very old material printed on poor quality or deteriorating paper.

If you are dissatisfied with the reproduction quality of any document that we provide, particularly those not exhibiting any of the above conditions, please feel free to contact our Directorate of User Services at (703) 767-9066/9068 or DSN 427-9066/9068 for refund or replacement.

END SCANNED DOCUMENT